Digest Journal of Nanomaterials and Biostructures

Dig. J. Nanomater. Bios. **2026**; 21(3): 51994
https://doi.org/10.31083/DJNB51994

Original Research

Multifunctional Bioactivity and Other Properties of Silver Nanoparticles Synthesized in an Eco-Friendly Manner From *Padina pavonica*

Kishori Battini[1,*,†], Venkata Mrunalini Nunna[1,†], Venkata Neelima Kotturu[1], Neelima Pannem[2], Usha Rayalcheruvu[1], Sainath Sri Bhashyam[3,4,*]

[1]Department of Biotechnology, Sri Padmavati Mahila Visvavidyalayam (Women's University), 517 502 Tirupati, Andhra Pradesh, India
[2]Department of Computer Science Engineering, School of Engineering and Technology (CSE, SoET), Sri Padmavati Mahila Visvavidyalayam (Women's University), 517 502 Tirupati, Andhra Pradesh, India
[3]Department of Biotechnology, Vikrama Simhapuri University, 524 324 Nellore, Andhra Pradesh, India
[4]Department of Food Technology, Vikrama Simhapuri University, 524 324 Nellore, Andhra Pradesh, India
*Correspondence: battinikishori@gmail.com (Kishori Battini); drsainath@vsu.ac.in (Sainath Sri Bhashyam)
[†]These authors contributed equally.
Academic Editors: Karol Kyzioł and Carmen-Georgeta Ristoscu
Submitted: 17 March 2026 Revised: 27 May 2026 Accepted: 5 June 2026 Published: 4 September 2026

Abstract

Background: This study focuses on the bioactivity and other properties of silver nanoparticles (AgNPs) synthesized using the ethanolic and methanolic extracts of *Padina pavonica*—a brown alga rich in phytochemicals capable of reducing metal ions and boosting the biological activity of biogenic AgNPs. **Methods:** AgNPs were characterized using ultraviolet–visible spectroscopy, dynamic light scattering (DLS), zeta potential measurements, scanning electron microscopy (SEM), Fourier transform infrared spectroscopy (FTIR), and X-ray diffraction (XRD). Phytochemicals in ethanolic and methanolic extracts were identified using gas chromatography-mass spectrometry. Antibacterial, antifungal, antioxidant (free radical scavenging, superoxide anion scavenging, and total antioxidant), and *in vitro* α-glucosidase inhibition (antidiabetic) activities were evaluated using the corresponding assays. Cytotoxicity was tested using the TM3 cell line. Molecular docking studies were conducted to investigate the interactions of major phytochemicals with bacterial and fungal targets. **Results:** Ultraviolet–visible spectra showed a characteristic surface plasmon resonance peak at 350–500 nm, confirming AgNP formation. DLS and zeta potential analyses indicated a nanoscale size distribution and good colloidal stability, SEM revealed a predominantly spherical particle morphology, FTIR spectroscopy identified functional groups involved in nanoparticle synthesis, and XRD revealed a crystalline structure. The identified bioactive phytochemicals included 2,4-Di-*tert*-butylphenol, ethyl oleate, hexadecanoic acid ethyl ester, octadecanoic acid, ergosterol and *n*-hexadecanoic acid (palmitic acid). Both ethanolic and methanolic extract–derived AgNPs exhibited high activity against *Bacillus subtilis*, *Staphylococcus aureus*, *Pseudomonas aeruginosa*, and *Salmonella enterica serovar Typhi (S. typhi)*, whereas activity against *Candida albicans* and *Aspergillus niger* was observed only for methanolic extract–derived AgNPs. Strong antioxidant and α-glucosidase inhibitory activities comparable with those of ascorbic acid and acarbose, respectively, were observed for biogenic AgNPs. TM3 cell line studies demonstrated high viability at a low concentration (3.125 mg/mL) of ethanolic AgNPs, indicating good biocompatibility. Molecular docking revealed that 2,4-Di-*tert*-butylphenol and chalcone engaged in stable interactions with microbial targets through hydrogen bonding, van der Waals, and π–π interactions. **Conclusion:** *P. pavonica* extract–derived AgNPs represent a promising eco-friendly nanoplatform with potential applications as antibacterials, antidiabetics, and antioxidants. The results of *in silico* studies corroborate the potential bioactivity of the selected bioactive phytochemicals, warranting further *in vivo* and clinical investigations.

Keywords: algae; antibacterial; antidiabetic; antifungal; antioxidant; green synthesis; *Padina pavonica*; silver nanoparticles

1. Introduction

During the recent past, the importance of nanotechnology has been well recognized as it plays a key role in distinct fields such as agriculture, food industry, cosmetics, and therapeutics [1,2,3]. The development of multifunctional scaffolds for bone tissue regeneration using 3D-printed polycaprolactone-magnetic nanoparticles composites [4], platinum based nano enzymes to treat intracerebral hemorrhage [5] and carrier-free nanoparticles based on natural products gambogic acid and glycyrrhizic acid to enhance phytotherapy against liver cancer [6] collectively exemplify the expanding role of nanotechnology in advanced biomedical applications. Further, experiments of Lu et al. [7], showed that the nanocomposites prepared from antimonene and copper ions efficiently produce bimetallic catalysts that degrade p-nitrophenol, a common toxic industrial pollutant is one of the cogent examples of exploration of nanotechnology to address environmental pollution problems.

Nowadays, significant attention towards the green synthesis of nanoparticles using phytocompounds and their therapeutic approaches is one of the promising research areas of nanotechnology [8,9]. In general, traditional methods like top-down and bottom-up approaches are used for the synthesis of nanoparticles, however due to adverse effects not only associated with high production cost, maintenance of physical conditions such as high pressure and temperature but also comprised of wide usage of toxic reducing agents as capping agents which lead to environmental pollution. These aspects evidently demanded eco-friendly and cost-reduction approaches that would allow new avenues to develop environmentally reducing and compatible solvents [10].

In the current scenario, green synthesis is believed to be one of the eco-friendly approaches wherein plant compounds are used as reducing and capping agents to fabricate nanoparticles. It is well known that the phytochemicals harbor a range of medicinal properties. For example, polysaccharides of *Alpinia zerumbet (Pers.)* and *Alocasia cucullata* and algae *Spirulina platensis* have been reported to exhibit medicinal properties such as anti-inflammatory [11], immune boosting abilities [12] and hypoglycemic effects on the type 2 diabetes [13]. Studies have shown that the potential of phytochemicals is elaborated at nanoscale size during fabrication of nanoparticles is one of the added advantages. Studies of Zu-Man et al. [14] reported that biogenic selenium nanoparticles stabilized by blackberry polysaccharides showed regulation of glucose and lipid metabolism in HepG2 cell lines, suggesting that these nanoparticles offer a promising nutritional approach to manage metabolic disorders [14].

Among the nanoparticles, silver nanoparticles (AgNPs) are widely used as antibacterial, antifungal, antiviral and anti-cancerous agents. Though AgNPs are promising, their ability to oxidize the surface of biological fluids in the presence of aerobic environment as it may lead to undesirable toxicity [15]. Nowadays, the role of plant and algal compounds in the biogenic synthesis of AgNPs and biomedicinal properties are well acknowledged. Published reports have shown that green synthesis of AgNPs using *Glycyrrhiza glabra* root extract showed antimicrobial activities against bacteria and fungi [16]. Studies also indicated that the biofabricated AgNPs using marine algae, *Ulva lactuca* exhibited antimicrobial, antidiabetic and antioxidant properties [17]. Recently, studies of Wang et al. [18] have shown that the multifunctional polyvinyl alcohol (PVA) hydrogel strain sensor reinforced by polydopamine/silver-decorated cellulose nanofibrils (PDA@CNF-Ag) fabricated via freeze-thaw process exhibits great potential as soft, skin-comfortable strain sensors in wearable electronics and personalized health monitoring devices. This finding elaborates the significance of phytochemical-based AgNPs beyond medicinal field [18].

In the current study, we explored a brown alga, *Padina pavonica* (family: Dictyotaceae) which is popularly known as marine brown alga in the biofabrication of AgNPs. *P. pavonica* is considered as rich biodiversity due to their wide array of biomedical properties and bio-indicator of environmental pollution. This brown alga is available from Atlantic, mediterranean, pacific and Indian oceans and grows in mangrove roots, rocks, shells, sea grass meadows, coral reefs, and littoral and shallow infralittoral zones, as well as beneath mudstone and sandstone cliffs [19]. Studies have shown that *P. pavonica* acts as an effective bioindicator of chemical pollution [20]. Further, the importance of this brown alga as fodder, bio-fertilizer, and plant growth promoter is well acknowledged [21]. At the perspective of health care aspects, *P. pavonica* exhibits antibacterial [22], anticancerous [23,24], antioxidant [25,26]. Moreover, insecticidal property of *P. pavonica* is also one of the cogent examples of environmentally benign biopesticides. Recent studies of Mesripour et al. [27] demonstrated the protective effects of *P. pavonica* against depressive behaviour in mice followed by dexamethasone exposure. These activities of *P. pavonica* at least in part might be ascribed to the occurrence of several bioactive compounds. Moreover, it has been stated that the major chemical classes of compounds found in *Padina* species comprised of polysaccharides, carotenoids, polyphenols, fiber, sterols and lipids [28]. Moreover, different solvents such as methanol, ethanol, ethyl acetate, hexane and water used in the extraction process may lead to extraction of different biochemical components from plants and algae owing to their solvent polarity [28].

In view of the aforementioned data, this study aims to integrate physicochemical characterization, biological activity assessment, *in silico* analysis, and cellular evaluation of green-synthesized AgNPs derived from *Padina pavonica*. To accomplish this task, we investigated, (a) characterization studies of green synthesis of AgNPs using ethanolic and methanolic extracts of *P. pavonica* using spectroscopic analysis, dynamic light scattering (DLS), Zeta potential, Fourier transform infrared spectroscopy (FTIR), scanning electron microscopy (SEM) and X-ray diffraction (XRD) analysis, and further, gas chromatography-mass spectroscopy (GC-MS) analysis of extracts of *P. pavonica* was performed to identify solvent based bioactive compounds, (b) evaluation of antibacterial, antifungal, antidiabetic and antioxidant activities of biosynthesized AgNPs using *P. pavonica*. Additionally, cytotoxic studies of the ethanolic extract of *P. pavonica* AgNPs were also performed. Finally, (c) we employed *in-silico* docking analysis of the solvent based phytochemicals identified through GC-MS against the targeted ligands of bacteria. TM3 cell lines are Mouse Leydig cell lines that are used widely for therapeutic and toxicological studies to understand the effect of chemical compounds on testosterone production. So far, studies associated with green synthesized AgNPs using

P. pavonica on Leydig cells (TM3 cell lines) did not report elsewhere. Further, studies aimed to investigate the cytotoxic effects of biogenic AgNPs on TM3 cell lines.

2. Materials and Methods

2.1 Procurement of Chemicals

The chemicals used in this study were of analytical grade and were procured from SD fine chemicals and Hi-Media, Mumbai, Maharashtra, India. The reagents related to the antioxidant activity were purchased from Sigma and Co., (St. Louis, MO, USA).

2.2 Sample Collection and Preparation

Padina pavonica was collected from the coastal areas of Nellore [Latitude: 14.5068° N; Longitude: 80.1788° E] and authenticated (Herbarium number: 2025/117, collected in November, 2025) with the experts of RK Algae Project Centre, Mandapam, Ramanathapuram (Dist.) located in Tamil Nadu state, India. This algal species is not listed under the International Union for Conservation of Nature (IUCN) and hence, not endangered. After collection, the alga was thoroughly washed twice with freshwater followed by distilled water to remove sand, salt and debris remnants. This step precedes shade-drying of washed *P. pavonica* and after confirmation, it was finely grounded into powder by using an electric mixer (**Supplementary Fig. 1)** and stored in zip-lock plastic bags for further analysis.

2.3 Preparation of Ethanolic and Methanolic Extracts

Padina pavonica powder was used for solvent extraction using ethanol (C_2H_5OH, ≥90% purity; CAS 64-17-5; Cat. No. 459844) and methanol (CH_3OH, ≥99.8% purity; CAS 67-56-1; Cat. No. 322415) solvents. Briefly, 10 g of powdered sample was added to 100 mL of each solvent separately, and soaked for 24–72 hours followed by the stirring about 20–30 min at 600–1000 rpm, and then subjected to filtration by using Whatman No.1 filter paper. The filtered ethanolic and methanolic extracts was kept in dark closed bottles separately and stored at 4 ℃ for further analysis.

2.4 Phytochemical Analysis of Extracts

Freshly prepared and filtered ethanolic extracts of *P. pavonica* (EPP) and methanolic extract of *P. pavonica* (MPP) were qualitatively analysed for the presence of phytochemicals such as alkaloids, flavonoids, saponins, tannins, terpenoids, steroids, carbohydrates, and proteins using the standard methods.

2.5 GC-MS Analysis

GC-MS analysis was performed to determine the chemical constituents present in the ethanolic and methanolic extracts which follows the methodology given by Sudha & Balasundaram [29] with slight modifications. Before analysis, the filtrates obtained in the previous step were again subjected to re-filtration using 0.22 µm syringe filters. Bio-active compounds present in solvent extracts was determined using GC-MS analysis (Shimadzu Corporation, Kyoto, Japan) [Model: Shimadzu, QP 2010 SE; Conditions: Capillary column (e.g., Durabond-5 Mass Spectrometry (DB-5MS), length: 30 m × diameter: 0.25 mm, thickness: 0.25 µm) and carrier gas: helium gas (purity: 99.99 %); constant flow rate of 1 mL/min]. GC-MS spectral detection was analysed using ionization energy of 70 eV with scan interval time of 0.2 s and fragments ranging from 40 to 600 m/z. The injection volume of 1 µL was used with a splitless mode and the injector temperature was maintained at 250 °C. The column oven temperature was maintained at 60 °C for 2 min, raised at 10 °C/min up to 200 °C then hold for 5 min and finally, the temperature was increased to 300 °C for 10 min. The phytochemicals in the ethanolic and methanolic extracts were identified based on comparison of their retention time, peak area and height and mass spectral patterns against spectral database of authentic Phyto-compounds available in the National Institute of Standards and Technology (NIST) library.

2.6 Biogenic Synthesis of AgNPs Using Padina pavonica Extracts

Solvent extracts of *P. pavonica* were used in the biofabrication of AgNPs where in silver nitrate ($AgNO_3$; CAS 7761-88-8; Cat. No. MB083) undergoes a bio-reduction reaction in the presence of phytochemicals [30]. Briefly, the algal extracts (10 mg) of ethanol and methanol were added to 1 mM silver nitrate solution in 1: 10 proportion separately. The reaction mixture was incubated in dark environment for a whole day or 24 h at room temperature to avoid the photo-activation of silver ions. The reduction of Ag^+ ions by phytoconstituents in the extracts resulted in a recognisable colour shift from green to light brown or colourless, signifying the successful synthesis of AgNPs visually. After synthesis, the reaction mixture was subjected to centrifugation at 12,000–15,000 rpm for 15 min to separate the synthesized silver nanoparticles and then the collected pellet was washed 2–3 times repeatedly with distilled water and ethanol to remove residual impurities and unreacted biomolecules. The purified nanoparticles were then dried in a hot air oven at 60 °C and stored for further characterization and biological evaluation. If the suspension is needed for such characterisation or evaluation, then again, the powdered nanoparticles are suspended in respective solvents as per the clearly selected concentrations.

2.7 Characterization of Biosynthesized AgNPs

Characterization of bio-synthesized nanoparticles is one of the important steps before deriving its biological applications. In the current study we employed multifaceted analytical techniques to characterize the bio-synthesized AgNPs. Ultra violet (UV)-visible spectrophotometry (Shimadzu Corporation, Kyoto, Japan) was the basic and most used to assess the ability of ethanolic and methanolic ex-

tracts of *P. pavonica* to reduce silver nitrate to AgNPs based on their optical properties. This technique provides valuable information towards the particle's size, shape and material composition based on the magnitude, peak wavelength and spectral bandwidth associated with AgNPs. The reduction of pure silver ions in the presence of plant capping agents were monitored by measuring the absorbance spectrum between wavelength range of 180 to 1100 nm. Scanning electron microscopy (SEM) (EVO MA 10, Carl Zeiss Microscopy GmbH, Jena, Germany) was used to analyse the size and morphology of the biosynthesized AgNPs, while energy–dispersive X–ray spectroscopy (EDS) analysis complements the SEM analysis by providing the elemental composition of AgNPs. Analysis of AgNPs using Zeta potential (Zetasizer Nano series) provides the electrostatic repulsion between the biosynthesized AgNPs and their stability, while their size distribution was analyzed through DLS experiments. DLS can even analyse through the Brownian motion of the particles in colloidal suspensions through the fluctuations observed in scattered light intensity. FTIR (ALPHA II, Bruker Optics GmbH & Co. KG, Ettlingen, Germany) is another important technique that gives insights into the identification of molecular structures and the characterization of chemical bonds in biosynthesized nanoparticles. The chemical bond vibrations reflect the occurrence of specific functional groups and the chemical environment that surrounded AgNPs. The crystalline nature and phase purity of biogenic AgNPs was analysed through X-ray diffraction method (XRD; Malvern PANalytical, Aeris advanced benchtop X-ray diffractometer, Almelo, Overijssel, Netherlands). The XRD pattern of the nanoparticles was recorded using a CuKα radiation source (λ = 1.5406 Å) under operating conditions of 40 mA in 2θ/θ scanning mode. The diffraction data were collected over a 2θ range of 10°–80°. For XRD analysis, the synthesized AgNPs were isolated by centrifugation followed by washing step with distilled water and ethanol to remove excess unreacted phytochemicals. The purified nanoparticle pellet was subsequently dried prior XRD analysis.

2.8 Biological Activities

2.8.1 Antibacterial Activity

Antibacterial property of the biosynthesized AgNPs from ethanolic and methanolic extracts of *P. pavonica* was individually determined through agar well diffusion method [31,32] at different concentrations (60, 80, 100, 120 µg/mL) against Gram-positive and Gram-negative bacteria strains such as *Bacillus subtilis*, *Staphylococcus aureus*, *Pseudomonas aeruginosa* and *Salmonella enterica serovar Typhi (S. typhi)*. Respective controls were maintained accordingly. All the plates were incubated at 37 °C for 24 h and the zone of inhibition around wells was measured using ImageJ (version 1.54, National Institutes of Health (NIH), Bethesda, Maryland, USA).

2.8.2 Antifungal Activity

The antifungal property of the silver nanoparticles from both the ethanolic and methanolic forms was determined using well diffusion method [33,34]. Different concentrations (60, 80, 100, 120 µg/mL) of AgNPs of *P. pavonica* was used to determine the antifungal activity against fungal species such as *Candida albicans* and *Aspergillus niger*. All the plates were incubated at room temperature that is 25–30 °C for 24–72 h and the zone of inhibition was measured using ImageJ.

2.9 Antioxidant Assays

The antioxidant potential of biogenic AgNPs synthesized from ethanolic and methanolic extracts of *P. pavonica* were evaluated by determining their ability to scavenge free radicals, superoxide anions and total antioxidant activity.

2.9.1 DPPH Scavenging or Free Radical Scavenging Activity

The free radical scavenging activity of the synthesized AgNPs was determined by analysing their ability to block stable radical 2,2-Diphenyl-1-picrylhydrazyl (DPPH; CAS 1898-66-4; Cat. No. D9132) formation [35,36]. Different concentrations *viz*., 20, 50, 100, and 150 µg/mL of biosynthesized AgNPs and Ascorbic acid (standard positive control) were used in the current study. All the experiments were done with the ethanolic and methanolic AgNPs from *P. pavonica* and also Ascorbic acid concentrations were individually performed. Briefly, 1 mL of freshly prepared 0.1 mM DPPH (dissolved in methanol) was added to 1 mL of biosynthesized AgNPs/Ascorbic acid (1:1). This step was immediately followed by thorough vortexing and mixture was kept at room temperature for 30 mins in dark. The free radical scavenging activity was measured at 517 nm spectrophotometrically and compared against the negative control (DPPH alone). The DPPH free radical scavenging activity was determined by the formula as follows: % of DPPH inhibition: = [Ac – As] / Ac × 100, wherein Ac = absorbance of DPPH (Negative control); As = absorption of AgNPs or Ascorbic acid.

2.9.2 Superoxide Anion Radical-Scavenging Assay

The superoxide anion radical-scavenging effect was determined by the method of Nishikimi et al. [37]. The purple formazan formed by nitro blue tetrazolium (NBT; CAS 298-83-9; Cat. No. N6876) by reacting with the superoxide radicals produced from phenazine methosulfate–nicotinamide adenine dinucleotide (PMS-NADH) non-enzymatic system were measured spectrophotometrically. In this assay, the reaction mixture consists of NBT (1 mM) in phosphate buffer (0.1 M, pH 7.4), NADH (1 mM), PMS (0.1 mM) and different concentrations that is 20, 50, 100 and 150 µg/mL of AgNPs incubated at room temperature for 5 min and the absorbance was recorded at 560 nm. The inhibition percentage was calculated against a blank control

without the test sample. The ability to inhibit the generation of superoxide radicals was expressed in terms of percentage by using the formula: [Ac – As] / Ac × 100; where Ac was the absorbance of negative control (all reagents without test samples), and As represent absorbance of AgNPs/Ascorbic acid.

2.9.3 Total Antioxidant Capacity Assay

The total antioxidant capacity (TAC) was determined as per the methodology of Ahmed et al. [38]. The assay was based on the reduction of Mo (VI) to Mo (V) by the antioxidant compounds in the sample under acidic conditions, forming a green-coloured phosphomolybdenum complex. Briefly, to 0.3 mL of AgNPs at different concentrations (20, 50, 100 and 150 µg/mL) was mixed with 3 mL of phosphomolybdenum reagent {28 mM monosodium phosphate (NaH_2PO_4), 4 mM ammonium molybdate [$(NH_4)6Mo7O_{24}\cdot 4H_2O$] in 0.6 M sulphuric acid (H_2SO_4)}(Cat. No. P4869) and incubated in a boiling water bath at 95 °C for 90 min followed by cooling step at room temperature. The absorbance was measured at 695 nm against a blank or negative control (3 mL reagent). Ascorbic acid was used as a reference and the results were expressed as µg Ascorbic Acid Equivalent per mg of extract (µg AAE/mg extract) of dry weight of the sample. Firstly, use the Standard curve to obtain Ascorbic acid equivalent concentration (µg/mL) with the help of the formula C = (A_sample − c) / m. Then, the Final TAC calculation TAC = C V/M. Where, C = equivalent ascorbic acid concentration (µg/mL), V = volume of sample used in assay (mL) and M = mass of extract or AgNPs used (µg).

2.10 Antidiabetic Activity

Inhibition Assay for α-Glucosidase Activity

The α-glucosidase inhibitory activity of AgNPs was evaluated based on the ability of AgNPs to inhibit the enzymatic hydrolysis of p-nitrophenyl-α-D-glucopyranoside (pNPG; CAS 3767-28-0; Cat. No. N1377) to p-nitrophenol, a yellow-coloured compound [39]. Briefly, to 50 µL of AgNPs at various concentrations (20, 50, 100, and 150 µg/mL) was pre-incubated with 50 µL of α-glucosidase solution (1 U/mL in 100 mM phosphate buffer, pH 6.8) at 37 °C for 10 minutes. The enzymatic reaction was initiated by adding 50 µL of 5 mM pNPG solution prepared in phosphate buffer. The reaction mixture was then incubated at 37 °C for 20 minutes. To stop the reaction, 100 µL of 0.1 M sodium carbonate (Na_2CO_3) was added to the incubated mixture. The development of yellow colour due to the formation of p-nitrophenol was measured at 405 nm spectrophotometrically. Acarbose (1 mg/mL) was used as the positive control. Appropriate blanks (without enzyme) and negative controls (enzyme with no sample) were included. The percentage inhibition of α-glucosidase activity was calculated using the following formula: Inhibition (%) = [Ac – As] / Ac × 100. Wherein Ac = absorbance of negative control (enzyme and substrate without sample); As = absorbance of AgNPs or Acarbose. The IC_{50} value, representing the concentration of sample required to inhibit 50% of enzyme activity, was determined by plotting percent inhibition against sample concentration using nonlinear regression.

2.11 In Vitro Cytotoxic Studies

2.11.1 Cell Culture

The TM3 Leydig cell lines were obtained from the cell bank (No. 1440/2021-22) National Centre for Cell Science (NCCS, Pune University Campus, Ganeshkhind Road, Pune - 411007, India). The cell line was authenticated using STR profiling prior its arrival to the lab by Indian Institute, NCCS, Pune. The cell cultures supplied by the NCCS, Pune were mycoplasma free. During the maintenance of cell cultures, reverse transcription polymerase chain reaction (RT-PCR) was often performed to verify whether mycoplasma contamination might occurred or not. After confirmation, further experimentation was performed. The TM3 cells (Passage No - P314, NCCS, Pune, India) were cultured in RPMI1640 medium containing 10% foetal bovine serum (FBS; Lot No. QVP1404280; Sigma Chemicals Co., Ltd, Mumbai, Maharastra, India), and 1% antibiotic penicillin-streptomycin at 37 °C in a humid atmosphere with 5% CO_2 concentration. Upon reaching at least 70% cell growth, the cells were separated from the flask by trypsin (0.05%) and centrifuged at 1500 rpm for 5 min. The resulting precipitate was prepared in suspension, and the percentage of cells was specified by Neubauer chamber and Trypan Blue dye through microscopy. After non-contamination was confirmed, cells with a viability of more than 90% were used for the experiment.

2.11.2 MTT Assay

Firstly, 3×10^3 TM3 cells were seeded in 96 well plate containing RPMI 1640 Medium and incubated for 24 h. Initial wells were untreated and contain only TM3 cells with medium, which can be used as the control group. The other wells were treated with different concentrations of ethanolic crude and AgNPs synthesized from *P. pavonica*. A stock concentration was prepared by dissolving the powdered crude and AgNPs samples in a solvent mixture containing 50% DMSO and 50% distilled water, yielding a concentration of 250 mg/mL. To ensure minimal solvent interference in cell viability measurements, all subsequent working concentrations were prepared by serial dilution with distilled water, maintaining the final DMSO concentration below 0.2 % (v/v) in all assay wells. From the stock solution, four test concentrations were prepared in a two-fold serial dilution series that is 25 mg/mL, 12.5 mg/mL, 6.25 mg/mL and 3.125 mg/mL.

In this study, the cell viability was assessed after 24 h by the 3-(4,5-Dimethylthiazol-2-yl)-2,5-diphenyltetrazolium bromide (MTT) colorimetric assay.

Medium was removed and the cells were treated with the dilutions of sample and incubated for 24 h. After incubation the media was removed and 50 µL of the MTT solution (5 mg/mL; Sigma Aldrich) was added to each well (except for the media control wells) and then the plate was incubated for 2 hours in CO_2 (5%) incubator at 37 °C temperature (98% humidity) to allow MTT reduction by the metabolically active cells. After the incubation period, the MTT solution was washed twice with phosphate buffered saline (PBS), and 150 µL of solubilization solution (Dimethyl sulfoxide-DMSO) (Sigma Aldrich) was added to each well, then wrapped in Aluminum foil and placed on orbital shaker at 50 rpm for 15 mins, which can result in the dissolving of crystals in viable cells. Later, the absorbance was measured at 540 nm using a Multiskan (Thermofisher) microplate reader [40,41,42]. Next, the cell viability and cytotoxicity percentage were calculated by using the equation given below. Negative (untreated) control refers typically cells + vehicle (e.g., 0.1% DMSO).

$$\% \text{ of Viability} = \frac{\overline{\text{OD}}_{\text{treated sample}}}{\overline{\text{OD}}_{\text{negative control}}} \times 100$$

$$\% \text{ of Cytotoxicity} = 100 - \% \text{ Viability}$$

2.12 Molecular Docking/Simulation

Molecular docking analysis is one of the powerful tools to investigate the antibacterial compounds and their interactions with proteins that are essential for bacterial and fungal growth. Published reports have shown that 2,4-Di-*tert*-butylphenol (DTBP) could be one of the natural antibacterial compounds found in plants [43]. In this study, GC-MS analysis indicated that DTBP was commonly found in ethanol and methanol extracts of marine alga, *P. pavonica* and was selected as the test compound. Based on the literature [44,45] proteins that could play vital roles for bacterial growth such as 2W9H (*S. aureus*), 6UF6 (*B. subtilis*), 6SPC (*P. aeruginosa*) and 3FHV (*S. typhi*) were selected. Since, methanolic extracts of marine alga exhibited antifungal activity, we determined the possible interactions between chalcones (antifungal compounds [46]) and 1NMT (*C. albicans* [47]). Molecular docking analysis was carried out using Auto Dock Vina (version 1.2.0, The Scripps Research Institute, La Jolla, CA, USA) to evaluate the binding interactions between the selected ligands and target proteins (Grid Box Coordinates: 30 × 30 × 30 Å for bacterial proteins; 30 × 25 × 15 Å for fungal proteins). The three-dimensional structures of the target proteins were retrieved from the Research Collaboratory for Structural Bioinformatics Protein Data Bank (RCSB PDB) in PDB format. Protein preparation was performed using Auto Dock Tools, wherein crystallographic water molecules were removed, polar hydrogen atoms were added, and non-polar hydrogens were merged. Kollman partial charges were then assigned, and the prepared protein structures were converted and saved in PDBQT (Protein Data Bank Partial Charge (Q) & Atom Type (T)) format for docking simulations. The ligand molecules, namely DTBP (PubChem ID: 7311) and chalcone (PubChem ID: 637760), were obtained from the PubChem database in Structure Data File (SDF) format. Ligand preparation was conducted using Auto Dock Tools by converting the SDF files to PDB format followed by structural optimization. Hydrogen atoms were added, Gasteiger partial charges were assigned, and rotatable bonds were defined to allow conformational flexibility during docking. The optimized ligands were finally saved in PDBQT format. Docking simulations were performed using the prepared protein and ligand files, and the resulting binding conformations were evaluated based on binding affinity scores. The two-dimensional (2D) and three-dimensional (3D) protein–ligand interactions were visualized and analysed using Discovery Studio Visualizer (version 21.1.0, Dassault Systèmes BIOVIA, San Diego, CA, USA).

2.13 Statistical Analysis

Results were expressed as mean ± standard deviation (SD). All experiments were performed in triplicate except for the MTT cytotoxicity assay which was performed using five individual samples per group (n = 5). Statistical analysis was carried out using one-way analysis of variance (ANOVA) to evaluate differences among groups, followed by Tukey's post-hoc test for multiple comparisons. A value of $p < 0.05$ was considered statistically significant.

3. Results

3.1 Phytochemical Analysis

In the present study, phytochemical screening of the methanolic and ethanolic extracts of *Padina pavonica* revealed the presence of various secondary metabolites (Table 1, Ref. [48,49,50,51,52,53]). Both methanolic and ethanolic extracts contained bioactive compounds such as carbohydrates, flavonoids, tannins, and alkaloids, whereas saponins and steroids were negligible to absent in both extracts. In contrast, terpenoids were detected exclusively in the ethanolic extract and were not observed in the methanolic extract.

3.2 Characterization of Synthesized Silver NPs

Preliminary confirmation of formation of AgNPs was evident from the observed visible colour changes wherein, the light greenish coloured solution showed a shift to yellow colour (both ethanolic and methanolic extracts before nano synthesis: Fig. 1A) and light yellowish (both ethanolic and methanolic extracts after nano synthesis: Fig. 1B). UV–visible spectroscopic analysis revealed that the synthesized AgNPs exhibited characteristic surface plasmon resonance

Table 1. Phyto-chemical (qualitative) analysis of *Padina pavonica* extracts.

S. No.	Name of the test	Phytochemical detected	Ethanolic extract of *P. pavonica*	Methanolic extract of *P. pavonica*	Ref.
1.	Wagner's Reagent	Alkaloids	+++	+++	[48]
2.	Alkaline Reagent Test	Flavonoids	+++	+++	[49]
3.	Foam Test	Saponins	--	--	[50]
4.	Ferric Chloride Test	Tannins	++	++	[51]
5.	Salkowski's Test	Terpenoids	+	--	[48]
6.	Salkowski's Test	Steroids	--	--	[48]
7.	Fehling's Test	Carbohydrates	+++	+++	[51]
	Benedict's reagent		+++	+++	[52]
8.	Biuret Test	Proteins	+	++	[53]

+++, strongly present; ++, moderately present; +, weakly present; --, completely absent.

(SPR) absorption peaks at 414 nm (Fig. 1C) and 419 nm (Fig. 1D) for the ethanolic and methanolic extracts, respectively.

Zeta potential of biogenic AgNPs synthesized from ethanolic extracts and methanolic extracts was found to be –70.0 mV (Fig. 2A) and –43.1 mV (Fig. 2B) respectively, suggesting that the electrostatic repulsions in AgNPs synthesized from ethanolic extracts were greater as compared to the AgNPs synthesized from methanolic extracts of *P. pavonica*, thereby reducing particle aggregation and enhancing dispersion stability. DLS experiments revealed the size distribution of AgNPs wherein, AgNPs synthesized using ethanolic extract of *P. pavonica* shows an average particle size of 156.9 nm (Fig. 2C), while AgNPs synthesized using methanolic extract of *P. pavonica* extracts showed an average particle size of 212.4 nm (Fig. 2D) and moreover, the distribution of ethanolic AgNPs showed a symmetrical and sharper peak indicating uniform nanoparticles over AgNPs biosynthesized from methanolic extracts. The ethanolic extracts of synthesized AgNPs showed a polydispersity index (PDI) of 0.527, while methanolic extracts of synthesized AgNPs showed a polydispersity index of 0.914. We did observe a high PDI in AgNPs biosynthesized from methanolic extracts and could be ascribed to the biomolecule classes possessing different reducing potentials and steric capacities. They reduce silver ions at different velocities and wrap around the resulting cores unevenly. This competitive, multi-component capping naturally yields a highly diversified, multi-sized particle population rather than a single uniform size.

SEM analysis revealed that the AgNPs synthesized using the ethanolic (Fig. 3A) and methanolic (Fig. 3B) extracts of *P. pavonica* exhibited agglomerated particle clusters, which may be attributed to the reduction and stabilization of silver ions by bioactive compounds present in the algal extracts. Furthermore, Energy Dispersive X-Ray Spectroscopy (EDS) (or EDAX) spectroscopy confirmed the elemental composition and purity of the synthesized AgNPs, as evidenced by a strong characteristic signal for metallic silver at approximately 3 keV. Moreover, weak signals such as carbon, nitrogen and oxygen peaks were also visible in the spectrum between 0 to 1 keV in both the biogenic AgNPs prepared from both the extracts (Fig. 3). Though there is a minimal discrepancy between the results of DLS and SEM which we noticed that could be due to aggregation in solution and/or dry state. Whereas, EDS spectrum indicated that silver (Ag) was the predominant element, confirming silver nanoparticle formation. Trace elements such as carbon (C) and oxygen (O) originated from the phytochemical capping layer of *P. pavonica* extract, enhancing colloidal stability. Chlorine (Cl) was detected due to its marine origin, co-extracted during polar solvent extraction, possibly forming AgCl deposits on the nanoparticle surface. Nitrogen (N) likely stemmed from residual nitrate ions or nitrogen-containing compounds in the extract. These elements do not alter the Ag-dominated composition or biological activity of the synthesized silver nanoparticles.

FT-IR analysis was performed to identify the functional groups involved in the reduction of silver ions and the stabilization of AgNPs. The FTIR spectra are presented in Figs. 4,5, and the corresponding peak assignments are summarized in Table 2. FTIR spectrum of the crude ethanolic extract (Fig. 4A) and methanolic extract (Fig. 5A) of *P. pavonica* indicated occurrence of bioactive functional groups. The absorption peaks in crude ethanolic extracts were 1638.88, 1043.46, and 634.89 cm^{-1}corresponding to characteristic stretching bands of polyphenols and flavonoids (from broad O–H and aromatic C–H bands), terpenoids, esters, and glycosides (from carbonyl and C–O stretches), alkaloids and phenolic acids (from carbonyl and aromatic ring vibrations). The absorption peaks in crude methanolic extracts were 1639, 1015.47, and 634.46 cm^{-1}corresponding to characteristic stretching bands of O–H indicating strong hydrogen bonding, often found in phenolic compounds and alcohols, C=O/C=C stretch suggesting conjugated systems (like aromatic rings or amides), commonly found in flavonoids and proteins, C–O stretch reflecting the existence of glycosidic linkages or polysaccharides and aromatic C–H bend suggesting complex polyphenolic structures. On the other hand, FTIR analysis of AgNPs synthesized from ethanolic extracts of *P. pavonica* (Fig. 4B and Table 2) revealed functional groups

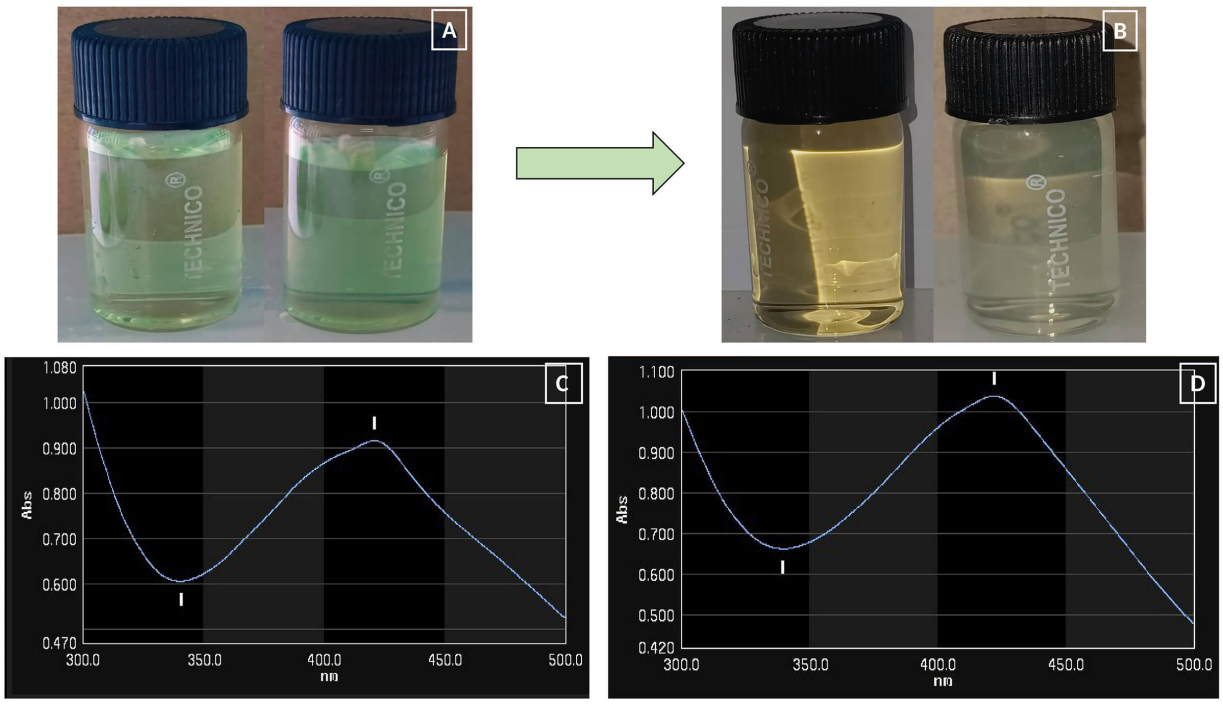

Fig. 1. Colour change observation of ethanolic and methanolic *Padina pavonica* extracts before nano synthesis (A) and after nano synthesis (B) respectively and Visible absorption spectra of silver nanoparticles synthesized from ethanolic (C) and methanolic (D) extracts of *Padina pavonica*, respectively.

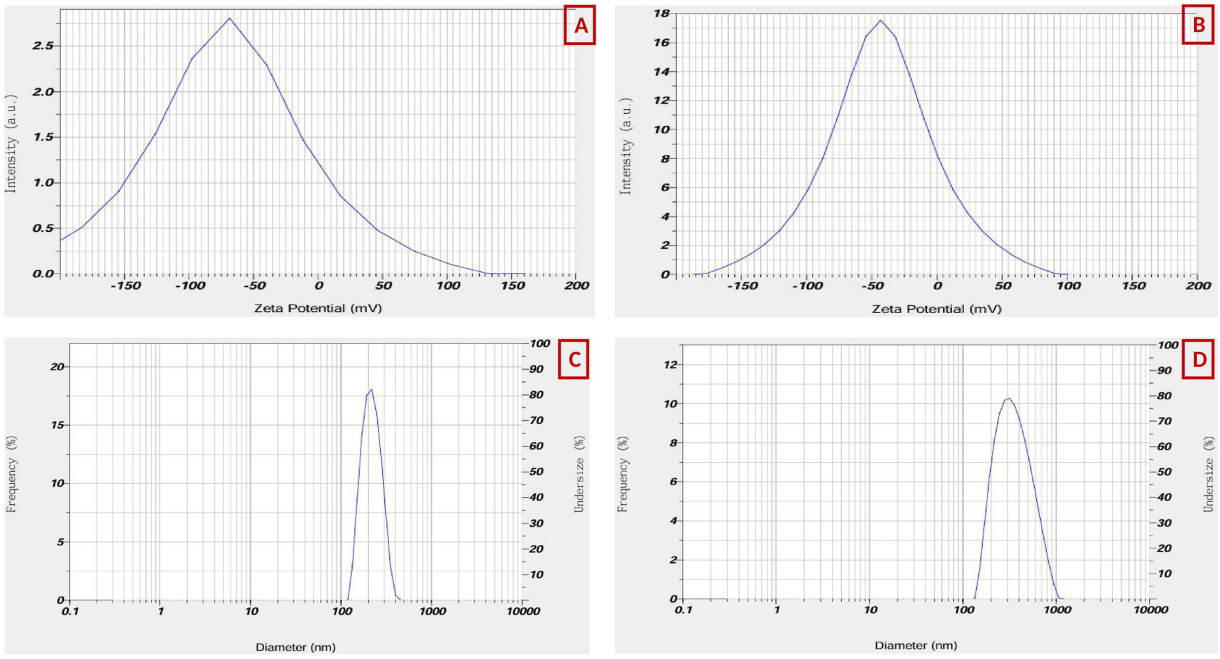

Fig. 2. Zeta-potential (ZP) of silver nanoparticles synthesized from ethanolic (A) and methanolic (B) extracts and Dynamic light scattering (DLS) of silver nanoparticles synthesized from ethanolic (C) and methanolic (D) extracts of *Padina pavonica*, respectively.

such as hydroxyl (–OH), carbonyl (C=O), alkane (C–H), ether/ester (C–O), and aromatic groups involved in the reduction of silver nitrate while FTIR analysis of AgNPs synthesized from methanolic extracts of *P. pavonica* (Fig. 5B and Table 2), revealed functional groups such as hydroxyl (–OH), carbonyl (C=O), alkane (C–H), ether/ester (C–O), and aromatic groups involved in the reduction of silver nitrate (Fig. 5B and Table 2).

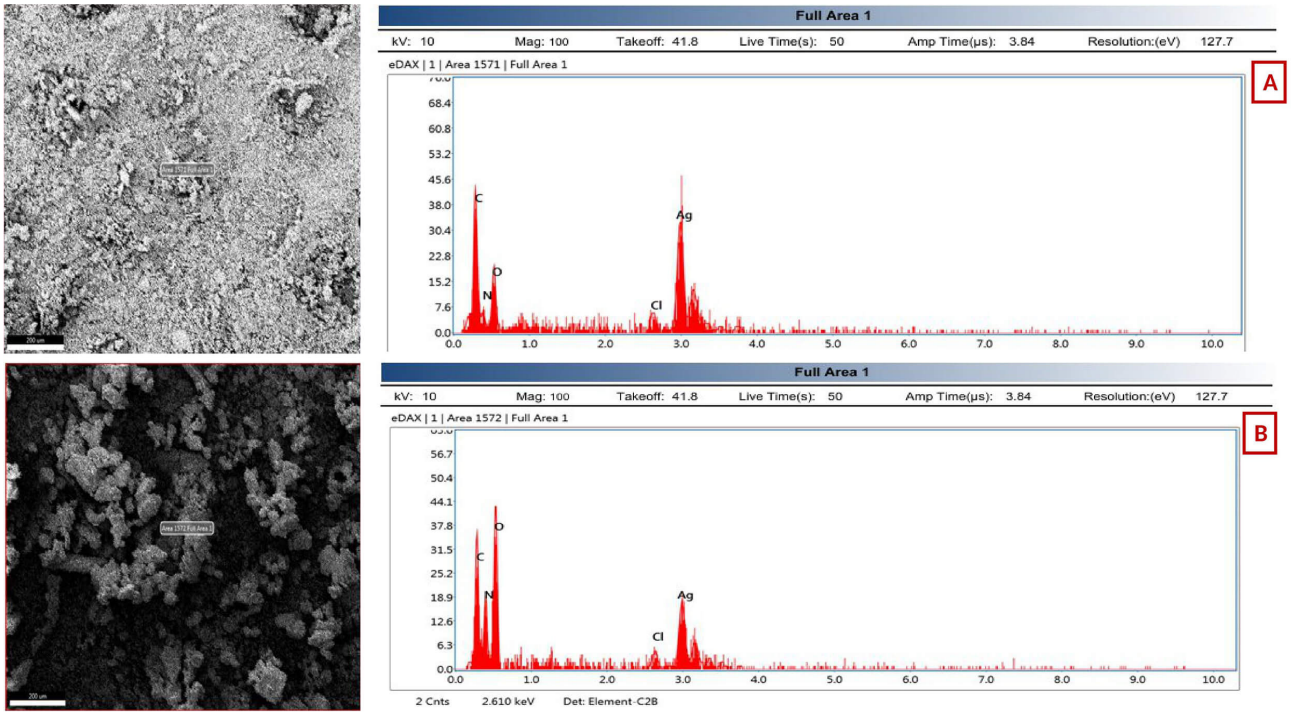

Fig. 3. Energy dispersive spectroscopy and scanning electron microscope images of silver nanoparticles synthesized from ethanolic (A) and methanolic (B) extracts of *Padina pavonica*. Scale bar = 200 μm.

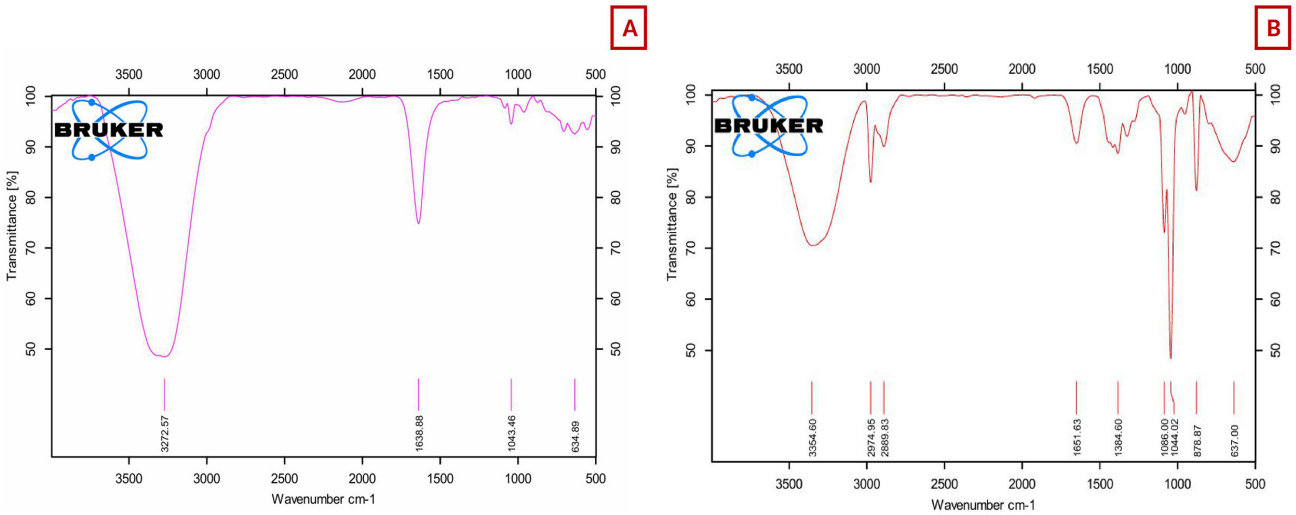

Fig. 4. Fourier transform infrared spectroscopy (FTIR) spectra of the crude (A) and silver nanoparticles (B) synthesized from ethanolic extracts of *Padina pavonica*.

XRD analysis of produced AgNPs synthesized from ethanolic extracts of *P. pavonica* showed prominent peaks at 14.17°, 27.79°, 28.71°, 29.33°, 32.19°, 38.09°, 44.16°, 46.10°, 47.83°, 48.30°, 54.76°, 57.42°, 59.72°, 64.41°, 67.38°, 74.40°, 79.08°, and 79.92° in Fig. 6A, while, XRD analysis of produced AgNPs synthesized from methanolic extracts of *P. pavonica* showed prominent peaks at 14.18°, 27.71°, 28.72°, 29.29°, 32.12°, 38.03°, 44.35°, 46.13°, 47.80°, 54.70°, 57.36°, 59.70°, 64.38°, 67.34°, and 77.23° in Fig. 6B. The diffraction peaks within the AgNPs synthesized from both the extracts of *P. pavonica* corresponded well with the standard database of the Joint Committee on Powder Diffraction Standards (JCPDS card No. 04-0783) (ICDD, Newtown Square, PA, USA), confirming the crystalline structure of the synthesized AgNPs. The sharp and intense diffraction peaks observed in the XRD patterns indicate a high degree of crystallinity in the AgNPs synthesized from both ethanolic and methanolic extracts of *P. pavonica*. In particular, the prominent peaks observed at 38.28° and 38.00° (2θ), respectively, were assigned to the domi-

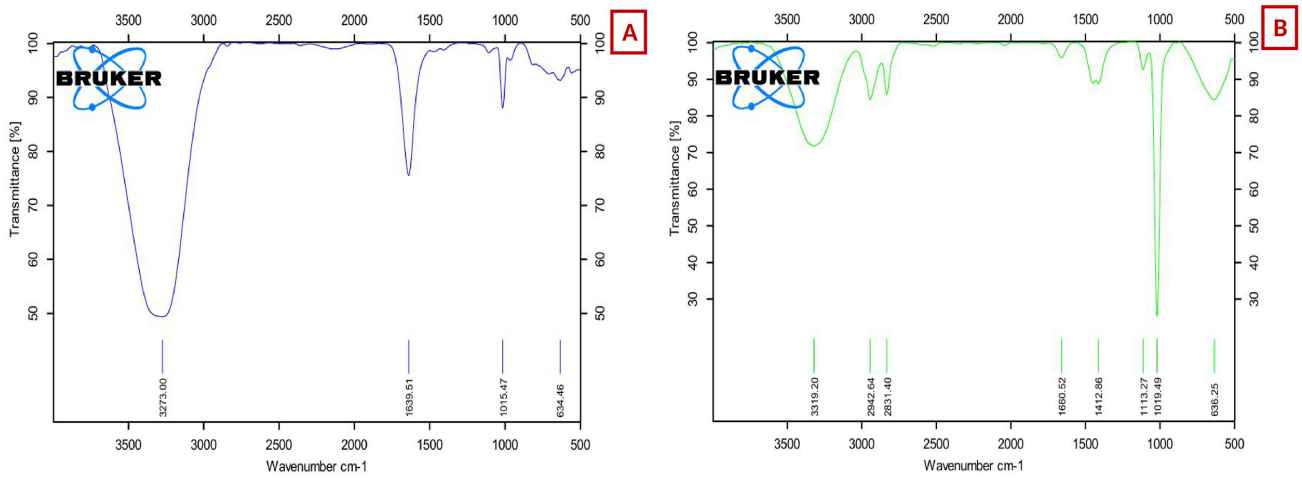

Fig. 5. FTIR spectra of the crude (A) and silver nanoparticles (B) synthesized from methanolic extracts of *Padina pavonica*.

nant crystallographic plane, suggesting a preferred orientation of the crystallites. Further, the majority of the indexed planes correspond well to the cubic silver chloride as per the JCPDS card No. 31-1238/85-1355, with specific facets originating from biomolecule-capped metallic silver. This confirms that the synthesis yielded a crystalline Ag and silver chloride nanocomposite, driven by the abundant chloride ions natively present within the algal matrix.

GC-MS analysis of biogenic AgNPs using ethanolic (Fig. 7) and methanolic (Fig. 8) extracts of *P. pavonica* indicated different peaks at various retention times.

All the peaks obtained via GC-MS analysis was analysed through library matching database e.g.: NIST (NIST 2020, National Institute of Standards and Technology, Gaithersburg, MD, USA) or Wiley libraries. Finally, GC-MS has revealed the presence of different metabolites in both ethanolic and methanolic extracts of *Padina pavonica* such as phenolic compounds, fatty acids, terpenoid and steroidal derivatives, and esters which strongly reported to possess antioxidant, antimicrobial, antidiabetic, and fertility-enhancing activities.

With respect to the ethanolic extracts of *P. pavonica* showed major compounds such as 2,4-Di-*tert*-butylphenol, Hexadecanoic acid ethyl ester, Octadecanoic acid, *n*-hexadecanoic acid (palmitic acid), Oleic acid, Ergosterol, Neophytadiene and Ethyl oleate, while with respect to the methanolic extracts of *P. pavonica* showed major compounds such as 2,4-Di-*tert*-butylphenol, Chalcone, n-hexadecanoic acid (palmitic acid), Benzyl benzoate, Pregnane-18,20-diol and 11-Ketoprogesterone.

3.3 Antibacterial and Antifungal Activity

Table 3 presents the antibacterial activity of AgNPs synthesized using ethanolic and methanolic extracts of *P. pavonica* at different concentrations (60, 80, 100, and 120 µg/mL) against selected Gram-positive and Gram-negative bacterial strains.

Based on the observed zones of inhibition, the phyto-synthesized AgNPs exhibited dose-dependent antibacterial activity against all tested bacteria, with antibacterial efficacy increasing as the concentration of AgNPs increased. Interestingly, antifungal activity against *A. niger* and *C. albicans* was obtained only with AgNPs synthesized from methanolic extracts of *P. pavonica* and were comparable against nystatin induced antifungal activity (Table 3). However, AgNPs synthesized ethanolic extracts from *P. pavonica* did not induce such antifungal activity. This difference between the methanolic and ethanolic extracts could be attributed the ability of more polarity of methanol to extract more polar phytochemicals. Zone of inhibition shown by ethanolic and methanolic extracts of *P. pavonica* against selected microorganisms were shown in (**Supplementary Figs. 2,3**).

3.4 Antioxidant Activity

Phyto-synthesized AgNPs using ethanolic and methanolic extracts of *P. pavonica* exhibited antioxidant properties as indicated by free radical scavenging activity, superoxide ion radical scavenging activity, and total antioxidant activity in a dose dependent manner (Table 4) and comparable against ascorbic acid induced antioxidant properties. AgNPs synthesized from ethanolic and methanolic extracts of *P. pavonica* showed antioxidant properties at selected concentrations 20, 50,100 and 150 µg/mL as compared to their respective controls at selected almost equivalent to controls. Furthermore, ethanolic AgNPs at 150 µg/mL exhibited a significant elevation in selected antioxidant properties as compared to methanolic AgNPs at the same concentration.

3.5 Antidiabetic Efficacy

α-Glucosidase inhibitory activity assay is one of the important indicators of antidiabetic property. AgNPs synthesized from ethanolic and methanolic extracts of *P.*

Table 2. FTIR spectra of crude and biofabricated silver nanoparticles of ethanolic and methanolic extracts of *Padina pavonica*.

Peak position (cm^{-1})	Functional group identified	Interpretation
Crude ethanolic extracts		
1638.88	Carbonyl (C=O) or Alkene (C=C)	This peak represents carbonyl groups (e.g., ketones, aldehydes, carboxylic acids) or C=C stretching in alkenes or aromatic rings. Suggests presence of terpenoids, flavonoids, or sterols.
1043.46	Alcohol or Ether (C–O) stretch	Confirms the presence of carbohydrates, glycosides, or esters, which are commonly found in marine algal extracts.
634.89	Aromatic C–H out-of-plane bending	Associated with aromatic rings; supports the presence of phenolic or flavonoid structures.
Crude methanolic extracts		
1639	Carbonyl (C=O) or Alkene (C=C)	Signifies presence of terpenoids, sterols, or flavonoid skeletons. Can also relate to amide groups (proteins).
1015.47	Alcohol or Ether (C–O) stretching	Associated with carbohydrates, esters, or glycosides—components often found in marine algae.
634.46	Aromatic or alkene substitution (C–H out-of-plane bend)	Confirms aromatic rings (flavonoids, tannins, phenolic acids).
Biosynthesized silver nanoparticles using ethanolic extracts		
3354.60 (broad)	–OH (Hydroxyl) group in alcohols or phenols	Indicates the presence of polyphenols, alcohols, or water molecules.
2974.95 and 2889.83	C–H stretching in alkanes	Presence of aliphatic chains or compounds like fatty acids or terpenes.
1651.63	C=O or C=C (Carbonyl or alkene group)	Suggests proteins (amide I band), ketones, aldehydes, or unsaturated compounds aiding in nanoparticle stabilization.
1384.60	C–H bending (Alkane) or O–H deformation (Phenolic)	Possibly due to methyl groups or phenolic content from the extract.
1086.00 and 1044.02	C–O stretch (Alcohol, Ether and Ester)	Indicates the presence of polysaccharides, glycosides, or esters – may play a role in capping and stabilizing AgNPs.
878.87 and 637.00	Aromatic C–H out-of-plane bend	Presence of aromatic compounds like phenols, flavonoids, or other secondary metabolites with aromatic rings.
Biosynthesized silver nanoparticles using methanolic extracts		
3319.20	–OH (Hydroxyl) group in alcohols or phenols	Indicates presence of phenolic compounds, alcohols or water, these compounds are key reducers and stabilizers during nanoparticle synthesis.
2942.64 & 2831.40	C–H stretching in alkanes	Presence of aliphatic chains or compounds like fatty acids or terpenes.
1660.52	C=O or C=C (Carbonyl or alkene group)	Suggests proteins (amide I band), ketones, aldehydes
1412.86	C–H bending, Alkane or O–H deformation	Possibly due to methyl groups or phenolic content from the extract.
1113.27 & 1019.49	C–O stretch (Alcohol, Ether and Ester)	Indicates the presence of polysaccharides, glycosides, or esters – may play a role in capping and stabilizing AgNPs.
636.25	Aromatic C–H out-of-plane bend	Presence of aromatic compounds like phenols, flavonoids, or other secondary metabolites with aromatic rings.

AgNPs, silver nanoparticles.

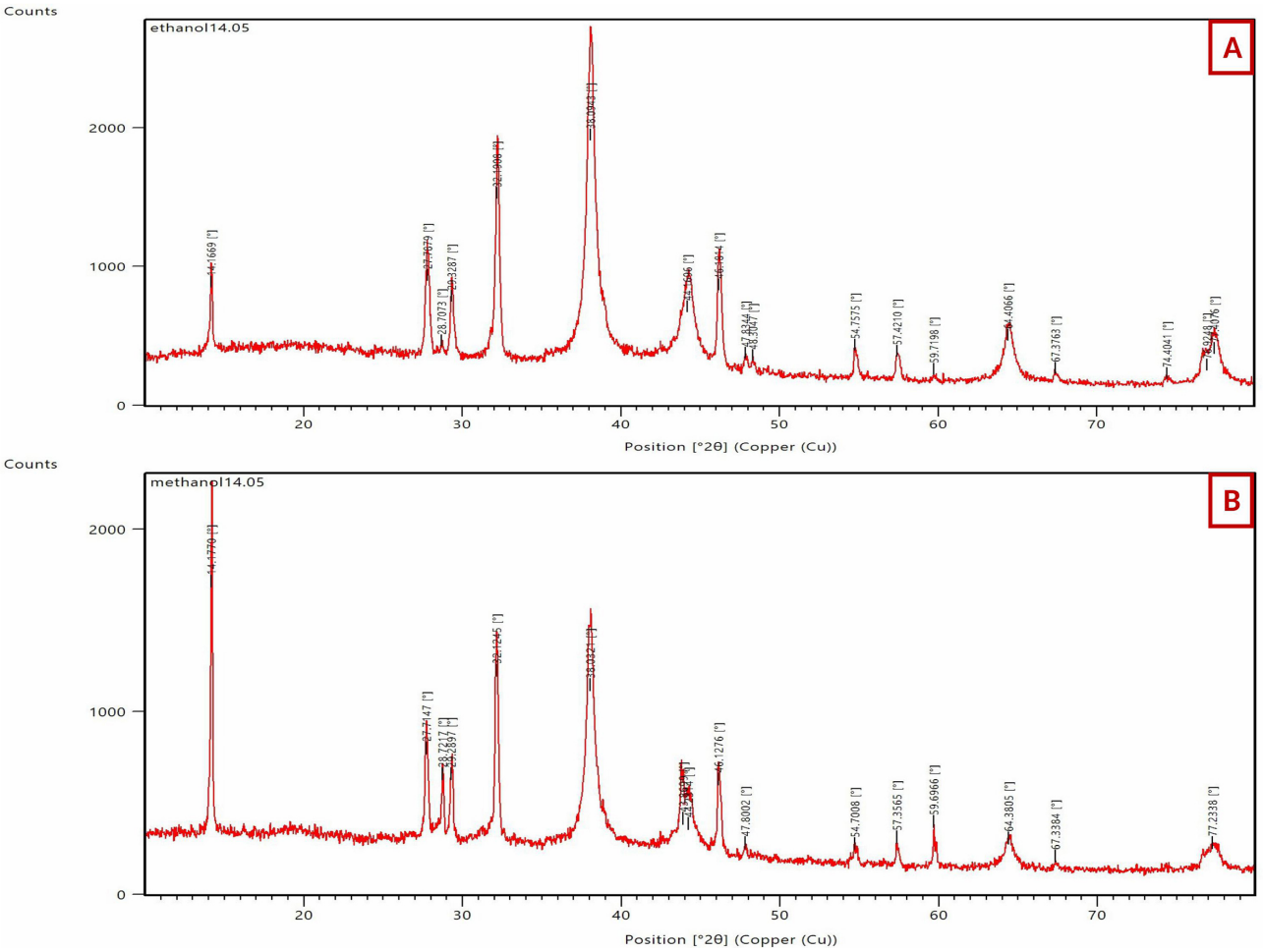

Fig. 6. X-ray diffraction spectra of silver nanoparticles synthesized from ethanolic (A) and methanolic (B) extracts of *Padina pavonica*.

pavonica exhibited antidiabetic activity as indicated by α-Glucosidase inhibitory activity assay at selected concentrations and the results were almost comparable to that of acarbose induced α- glucosidase inhibitory activity levels (Fig. 9). The results indicated that the AgNPs synthesized from ethanolic and methanolic extracts of *P. pavonica* exhibited IC_{50} values of 65.22 µg/mL and 71.50 µg/mL, respectively.

3.6 MTT Assay

Ethanolic extracts of crude and the AgNPs synthesized from *P. pavonica* exhibited clear cell proliferation and less cytotoxicity at selected concentrations. These results indicate that the test samples exhibited a dose-dependent cell proliferative and cytotoxic effects (Table 5), the nanoparticle formulations showed slightly higher cell viability compared with crude extracts, with maximum viability of 94.57% with less cytotoxicity of 5.43%. The results indicate significantly reduced cell proliferation at higher concentrations in both crude and nano tested samples compared with lower concentrations.

3.7 In Silico Analysis

Table 6 shows the binding affinities and interacted amino acids of selected bacteria and fungi against DTBP and chalcone, respectively. The docking analysis of DTBP with *Staphylococcus aureus* protein (PDB ID: 2W9H) revealed a binding affinity of −6.9 kcal/mol. The ligand formed a conventional hydrogen bond with Leu5, along with carbon–hydrogen bonds involving Leu5 and Val6. Hydrophobic interactions were observed with Leu28 (alkyl), Val31 (Pi–alkyl), Phe92 (Pi–Pi stacked and Pi–alkyl), and Phe98 (Pi–alkyl) residues, indicating stable accommodation of DTBP within the active site. DTBP showed a stronger binding affinity of −7.7 kcal/mol with *Bacillus subtilis* protein (PDB ID: 6UF6, A-chain). The interaction was stabilized by a conventional hydrogen bond with Gly219, in addition to extensive hydrophobic interactions, including Pi–Pi, alkyl, and Pi–alkyl interactions with Val69, Val92, Ile71, Ile88, Thr99, Ile257, Gln268, and Gln270. Multiple van der Waals interactions further contributed to the stability of the DTBP–6UF6 complex. In the case of *Pseudomonas aeruginosa* protein (PDB ID: 6SPC, B-chain), DTBP exhibited a binding affinity of −5.9

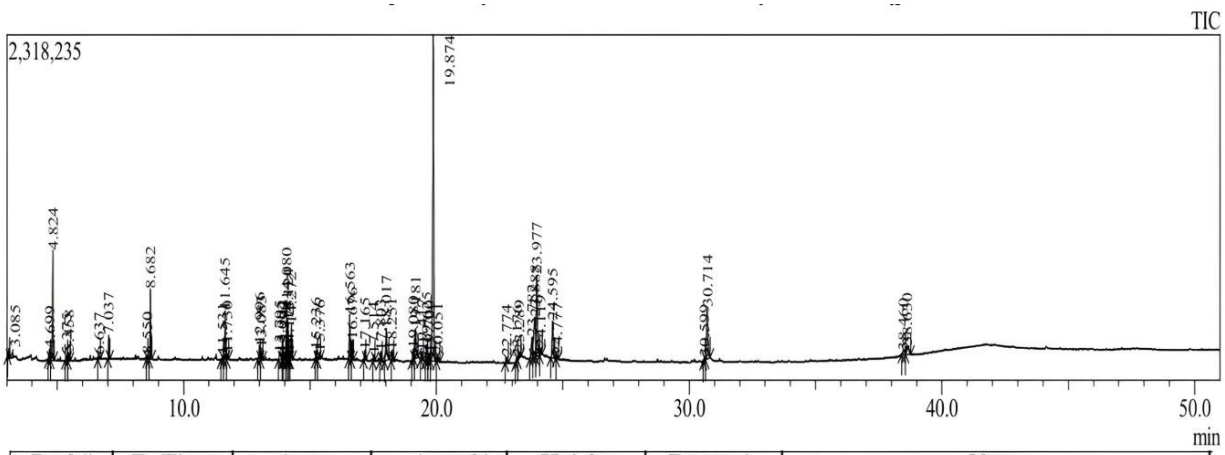

Peak#	R. Time	Area	Area %	Height	Base m/z	Name
1.	3.085	123161	0.52	61582	43.00	Dimethoxane
2.	4.699	182117	0.77	72633	103.10	Butane, 1,1-diethoxy-3-methyl-
3.	4.824	1343620	5.66	732822	61.05	Ethane, 1,1,1-triethoxy-
4.	5.375	142630	0.60	32715	57.10	Undecane, 1-bromo-
5.	5.458	186763	0.79	51738	57.10	Decane
6.	6.637	63799	0.27	23468	107.05	Propane, 1,1,3-triethoxy-
7.	7.037	229308	0.97	156165	73.10	(Methoxymethyl)trimethyl silane
8.	8.550	61765	0.26	27356	43.05	1-Dodecene
9.	8.682	873753	3.68	465424	57.10	Dodecane
10.	11.531	66284	0.28	30240	43.05	1-Tridecene
11.	11.645	715098	3.01	328204	57.10	Tetradecane
12.	11.730	74501	0.31	36233	105.10	N1-(2,5-Dimethylphenyl)-N2-(1-phenylethyl) oxamide
13.	12.996	203760	0.86	96632	57.10	Pentadecane
14.	13.083	138663	0.58	77859	191.20	2,4-Di-tert-butylphenol
15.	13.795	261115	1.10	42009	149.10	Diethyl Phthalate
16.	13.902	114240	0.48	43136	57.10	Pentadecane, 3-methyl-
17.	13.990	134999	0.57	37501	149.10	Diethyl Phthalate
18.	14.080	678578	2.86	399773	149.10	Diethyl Phthalate
19.	14.124	470494	1.98	259689	149.10	Diethyl Phthalate
20.	14.175	83177	0.35	45731	83.10	1-Hexadecanol
21.	14.272	494614	2.08	236560	57.10	Hexadecane
22.	15.236	116118	0.49	60890	196.10	Benzo[d]isothiazol-3-one, 2-(2-ethoxy-2-oxoethyl)-,1,1-dioxide
23.	15.376	103387	0.44	44138	55.05	2-Propenoic acid, tridecyl ester
24.	16.563	561781	2.36	299958	88.10	Tetra decanoic acid, ethyl ester
25.	16.676	228722	0.96	129747	57.10	Heneicosane
26.	17.165	124247	0.52	65213	68.10	Neophytadiene
27.	17.514	89023	0.37	41031	149.10	Neophytadiene
28.	17.803	144180	0.61	64100	82.10	Neophytadiene
29.	18.017	730609	3.08	214683	86.10	Lidocaine
30.	18.251	172675	0.73	70793	57.10	7,9-Di-tert-butyl-1-oxaspiro(4,5)deca-6,9-diene-2,8-dione
31.	19.080	191258	0.81	71041	73.05	n-Hexadecanoic acid
32.	19.181	659821	2.78	197545	73.10	n-Hexadecanoic acid
33.	19.417	156294	0.66	51927	55.10	Ethyl 9-hexadecenoate
34.	19.625	328163	1.38	106957	55.10	Ethyl 9-hexadecenoate
35.	19.700	150649	0.63	49793	118.15	Fumaric acid, cycloheptyl pentadecyl ester
36.	19.874	6416075	27.01	2188035	88.10	Hexadecanoic acid, ethyl ester
37.	20.051	121451	0.51	40765	57.10	Heneicosane
38.	22.774	112097	0.47	36179	99.10	Hexanoic acid, undec-2-enyl ester
39.	23.176	67614	0.28	22489	55.05	Oleic Acid
40.	23.289	122717	0.52	33616	55.05	Oleic Acid
41.	23.782	560672	2.36	138981	73.05	Octadecanoic acid
42.	23.888	1164778	4.90	263899	73.05	Octadecanoic acid
43.	23.977	2002403	8.43	541527	55.10	Ethyl Oleate
44.	24.119	161117	0.68	42857	55.10	Ethyl Oleate
45.	24.595	754756	3.18	245739	88.10	Octadecanoic acid, ethyl ester
46.	24.777	57142	0.24	21896	57.10	Heptadecane
47.	30.599	52944	0.22	21101	57.10	Myristic acid glycidyl ester
48.	30.714	1175189	4.95	345030	176.20	Benzyl diethyl-(2,6-xylylcarbamoylmethyl)-ammonium benzoate
49.	38.460	160590	0.68	18318	88.10	Heneicosanoic acid, 2,4-dimethyl-, methyl ester
50.	38.630	429476	1.81	54658	69.10	Ergosterol

Fig. 7. Gas chromatography-mass spectroscopy of ethanolic extract of *Padina pavonica*.

kcal/mol. The complex formation involved a conventional hydrogen bond with Asp153, hydrophobic Pi–alkyl interaction with Tyr91, and an electrostatic Pi–cation interaction with Lys152. Additional stabilization was provided by van der Waals interactions with Ala85, Arg86, Gly88, Met89, Pro90, and Gly150. Docking of DTBP with *S. typhi* protein (PDB ID: 3FHV, A-chain) resulted in a binding affinity of −6.2 kcal/mol. A conventional hydrogen bond and Pi–sigma interaction were formed with Asn180, while Ile47 participated in two alkyl and one Pi–alkyl in-

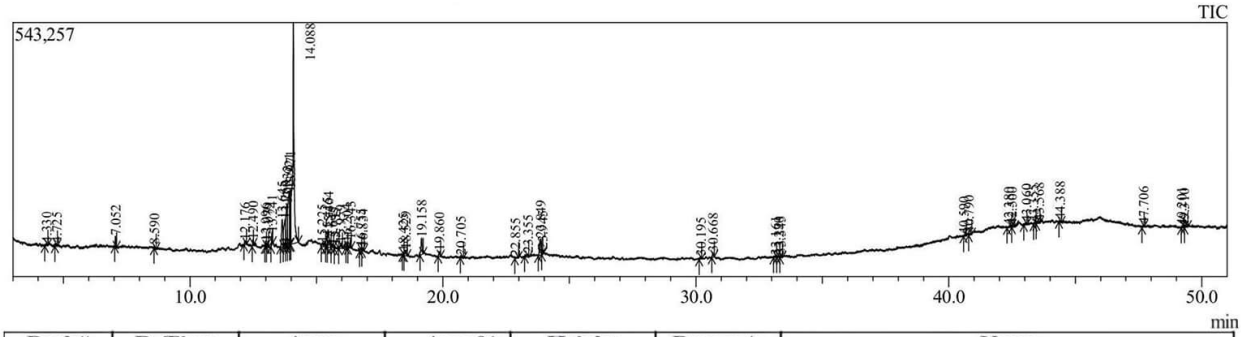

Peak#	R. Time	Area	Area%	Height	Base m/z	Name
1.	4.330	16612	0.34	3589	40.00	2,5-Furandione, dihydro-3-methylene-
2.	4.725	18312	0.37	4301	44.00	(S)-(+)-1-Cyclohexylethylamine
3.	7.052	33974	0.69	22461	57.10	Tetradecane
4.	8.590	16832	0.34	5911	120.10	Methyl salicylate
5.	12.176	27498	0.56	7760	71.10	Decane, 1-iodo-
6.	12.490	18632	0.38	11381	73.10	3-Isopropoxy-1,1,1,7,7,7-hexamethyl-3,5,5-tris(trimethylsiloxy)tetr
7.	12.996	17475	0.35	9815	85.15	Pentadecane
8.	13.079	22650	0.46	12298	191.15	2,4-Di-tert-butylphenol
9.	13.241	48505	0.98	25108	105.05	1,2-Propanedione, 1-phenyl-, 2-oxime
10.	13.645	211312	4.27	58179	149.10	Diethyl Phthalate
11.	13.760	234188	4.73	56569	149.10	Phthalic acid, monoethyl ester
12.	13.832	376232	7.61	87768	149.10	Diethyl Phthalate
13.	13.921	514538	10.40	111980	149.10	Diethyl Phthalate
14.	13.971	329053	6.65	117214	149.10	Diethyl Phthalate
15.	14.088	1835532	37.10	473155	149.10	Diethyl Phthalate
16.	15.225	55584	1.12	7018	44.00	Ethanol, 1-(2-methylene-1-phenylsulfonylcyclopropyl)-
17.	15.415	73451	1.48	22907	85.10	Sulfurous acid, hexyl nonyl ester
18.	15.464	163628	3.31	36522	85.10	2-Methylhexacosane
19.	15.645	22991	0.46	4250	97.10	Pregnane-18,20-diol, (5. alpha.)-
20.	15.735	18884	0.38	5148	87.10	Dodecanoic acid, 11-hydroxy-, methyl ester
21.	15.959	32748	0.66	9591	85.15	Methoxy acetic acid, 4-hexadecyl ester
22.	16.204	26548	0.54	10383	105.05	N-Benzyl-2-aminocinnamate, methyl ester
23.	16.343	46072	0.93	16654	105.10	Benzyl Benzoate
24.	16.755	25053	0.51	7747	71.10	Eicosyl nonyl ether
25.	16.834	16490	0.33	6336	44.00	Penta decanal-
26.	18.425	14232	0.29	6333	44.05	Eicosanal-
27.	18.529	38566	0.78	11797	87.10	Pentadecanoic acid, methyl ester
28.	19.158	120352	2.43	34291	73.05	n-Hexadecanoic acid
29.	19.860	35956	0.73	11122	88.10	Eicosanoic acid, ethyl ester
30.	20.705	13737	0.28	4715	45.05	3-(4-Amino-furazan-3-yl)-5-methyl-3H-[1,2,3]triazole-4-carboxyli
31.	22.855	14413	0.29	2786	40.00	11-Ketoprogesterone
32.	23.355	35748	0.72	6328	44.00	Trichloroacetic Acid
33.	23.849	140150	2.83	34088	73.10	Octadecanoic acid
34.	23.945	22991	0.46	9308	40.00	Ethanol, 2-(octyloxy)-
35.	30.195	17172	0.35	4942	44.05	1,2,4-Oxadiazole, 5-methyl-3-(1-piperidylmethyl)-
36.	30.668	27309	0.55	10007	98.10	Myristic acid glycidyl ester
37.	33.161	18436	0.37	4545	207.10	Phenol, 2,6-dichloro-4-nitro-
38.	33.270	13952	0.28	3561	207.05	Silane, chlorodiethylheptyloxy-
39.	33.345	17577	0.36	4950	44.05	Tricyclo [4.3.1.1(3,8)] undecan-1-amine
40.	40.590	13478	0.27	2833	44.05	3-Fluoroamphetamine
41.	40.790	13725	0.28	3271	207.10	Chalcone
42.	42.380	27594	0.56	4186	207.10	Acetamide, N-tricyclo [4.3.1.1(3,8)] undec-3-yl-
43.	42.500	21603	0.44	3944	207.10	1,2-Benzenediol, 3,5-bis(1,1-dimethylethyl)-
44.	43.060	19166	0.39	4917	44.05	2,3-Anhydro-d-mannosan
45.	43.355	17313	0.35	2948	207.10	3-tert-Butylphenol, trimethylsilyl ether
46.	43.568	22936	0.46	4313	44.05	Silicic acid, diethyl bis(trimethylsilyl) ester
47.	44.388	14175	0.29	4524	103.05	5-(7a-Isopropenyl-4,5-dimethyl-octahydroinden-4-yl)-3-methyl-pent-2-enal
48.	47.706	16606	0.34	4627	44.05	Thiosulfuric acid, S-(2-amino-1-phenylpropyl) ester
49.	49.201	18313	0.37	4883	44.05	1,2-Bis(trimethylsilyl)benzene
50.	49.310	28714	0.58	1063	73.10	Trimethylsilyl-di(timethylsiloxy)-silane
		4947008	100.00	1324327		

Fig. 8. Gas chromatography-mass spectroscopy of methanolic extract of *Padina pavonica*.

teraction. Several van der Waals interactions were also observed with Met50, Lys51, Phe110, Asn111, Asn112, Phe114, Gly138, and Tyr179, contributing to complex stabilization. Chalcone docking with *Candida albicans* protein (PDB ID: 1NMT, A-chain) demonstrated a binding affinity of −7.6 kcal/mol. The ligand formed a conventional hydrogen bond with Gly413 and exhibited strong Pi–Pi stacking interactions with Tyr225 and Phe240. Additional van der Waals interactions with Asp111, Asp112, Phe115, His227, Gly411, and Asp412 further stabilized the ligand within the active site. The docking interactions between the ligands and selected proteins of bacteria and fungi were shown in (**Supplementary Figs. 4–8**).

Table 3. Antimicrobial activity of bio-synthesized silver nanoparticles generated from ethanolic and methanolic extracts of *Padina pavonica*.

Zone of inhibition (in mm)					
Silver nanoparticles using ethanolic extracts at different concentrations					
	60 µg/mL	80 µg/mL	100 µg/mL	120 µg/mL	standard
B. subtilis	2.9 ± 0.12^{a}	3.1 ± 0.17^{b}	3.5 ± 0.2^{c}	4.5 ± 0.23^{d}	7.77 ± 0.32^{e}
S. aureus	2.1 ± 0.23^{a}	2.4 ± 0.23^{a}	3.5 ± 0.3^{b}	4.4 ± 0.34^{c}	10.0 ± 0.45^{d}
S. typhi	3.9 ± 0.5^{a}	4.5 ± 0.16^{b}	5.5 ± 0.23^{c}	6.0 ± 0.36^{d}	10.7 ± 0.16^{e}
P. aeruginosa	3.7 ± 0.19^{a}	4.0 ± 0.24^{ab}	4.4 ± 0.56^{b}	5.7 ± 0.46^{c}	6.73 ± 0.22^{d}
Silver nanoparticles using methanolic extracts at different concentrations					
B. subtilis	3.0 ± 0.51^{a}	3.5 ± 0.29^{b}	3.85 ± 0.68^{b}	5.4 ± 0.32^{c}	10.0 ± 0.15^{d}
S. aureus	3.9 ± 0.17^{a}	4.6 ± 0.18^{b}	4.9 ± 0.54^{b}	5.9 ± 0.26^{c}	11.8 ± 0.47^{d}
S. typhi	4.1 ± 0.14^{a}	4.5 ± 0.25^{ab}	5.2 ± 0.42^{b}	6.1 ± 0.18^{c}	12.7 ± 0.15^{d}
P. aeruginosa	4.5 ± 0.12^{a}	4.8 ± 0.34^{a}	5.4 ± 0.25^{b}	6.0 ± 0.24^{c}	13.0 ± 0.16^{d}
Silver nanoparticles using methanolic extracts at different concentrations					
C. albicans	6.4 ± 0.18^{a}	7.0 ± 0.46^{b}	10.0 ± 0.34^{c}	10.3 ± 0.56^{c}	12.0 ± 0.54^{d}
A. niger	9.5 ± 0.36^{a}	10.0 ± 0.36^{a}	10.5 ± 0.26^{b}	11.4 ± 0.28^{c}	12.0 ± 0.62^{c}

Values are expressed as mean ± standard deviation (SD) of three independent determinations (n = 3). Different superscript letters within the same row indicate statistically significant differences according to one-way analysis of variance (ANOVA) followed by Tukey's post hoc test ($p < 0.05$). Streptomycin (10 µg/mL) and nystatin (50 µg/mL) were used as standard antibacterial and antifungal controls, respectively.

Table 4. *In vitro* antioxidant efficacy of bio-synthesized silver nanoparticles (AgNPs) from ethanolic and methanolic extracts of *P. pavonica*.

Concentration (µg/mL)	Control	Ethanolic AgNPs	Methanolic AgNPs
DPPH radical scavenging activity (%)			
20	25.1 ± 1.24	22.7 ± 2.24	22.8 ± 2.23
50	49.8 ± 1.08	45.3 ± 2.94	44.2 ± 3.97
100	58.2 ± 0.88	55.1 ± 3.54	53.8 ± 2.54
150	60.9 ± 1.97	62.1* ± 3.24	55.2 ± 4.23
Superoxide anion radical scavenging activity (%)			
20	27.2 ± 0.98	25.1 ± 2.04	22.1 ± 2.63
50	40.7 ± 1.08	35.4 ± 2.69	34.4 ± 3.09
100	57.9 ± 1.05	56.2 ± 3.57	51.2 ± 2.93
150	73.3 ± 1.08	75.4* ± 3.53	66.7 ± 3.23
Total antioxidant activity (µg AAE/mg extract)			
20	12.2 ± 1.01	9.7 ± 2.12	8.8 ± 2.23
50	20.5 ± 1.09	17.3 ± 2.19	13.6 ± 1.72
100	31.2 ± 0.90	28.1 ± 3.23	28.8 ± 2.45
150	37.9 ± 1.10	41.3* ± 1.98	38.2 ± 1.23

Values are mean ± S.D. of triplicate experiments. For evaluation of '*p*' value for both ethanolic and methanolic AgNPs, control group served as controls. Mean values with asterisk superscript indicate statistically significant difference compared to control and AgNPs at the same concentration. *Significant at $p < 0.05$. µg AAE/mg extract, µg Ascorbic Acid Equivalent per mg of extract.

4. Discussion

In this study, we demonstrated the antibacterial, antifungal, antidiabetic and antioxidant properties along with the *in-silico* docking studies with respect to the selected ligand and proteins of eco-friendly fabricated silver nanoparticles using marine brown alga, *P. pavonica*. The major objective of this study was to develop eco-friendly capping agents which can able to reduce silver in an effective

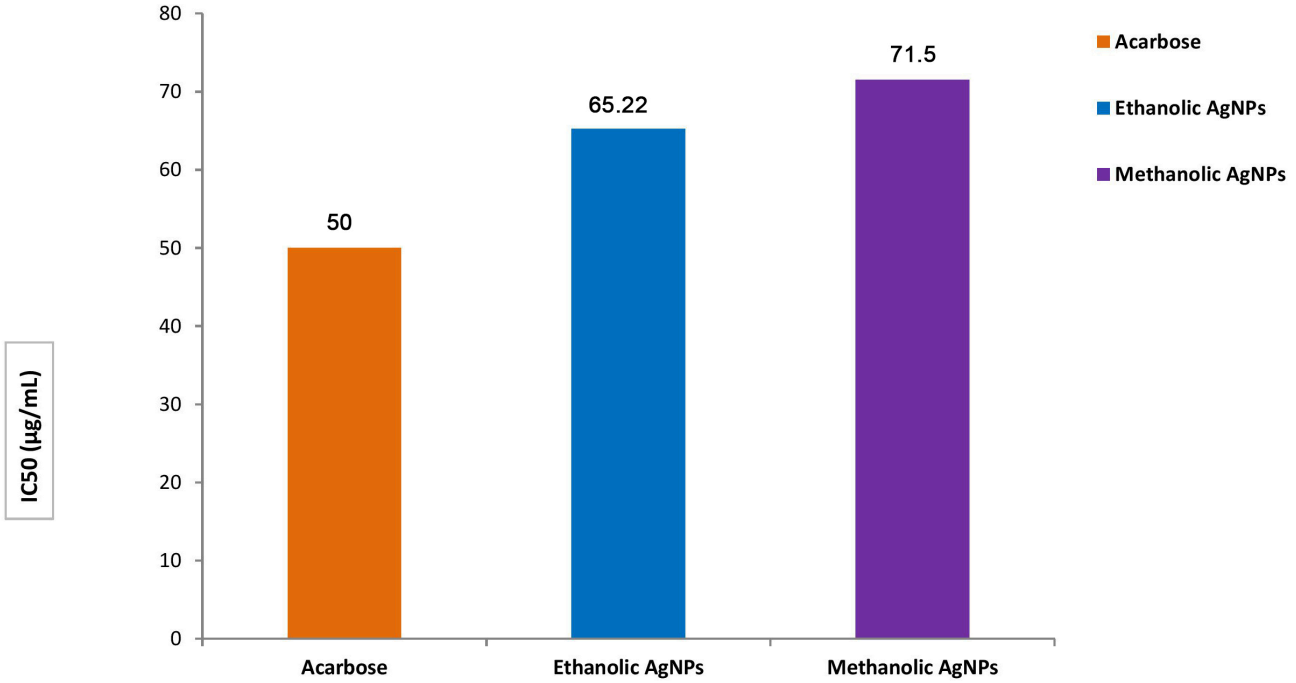

Fig. 9. IC_{50} values of *in vitro* antidiabetic effect of silver nanoparticles synthesized from both ethanolic and methanolic extracts of *Padina pavonica*.

Table 5. *In vitro* cytotoxic assay of crude and silver nanoparticles (AgNPs) synthesized from ethanolic extract of *P. pavonica* (EPP).

S. No	Groups	% of viability	% of cytotoxicity
1.	Control	100.00%	0.00%
2.	EPP_1 (25 mg/mL)	85.60%	14.4%
3.	EPP_2 (12.5 mg/mL)	90.54%	9.46%
4.	EPP_3 (6.25 mg/mL)	92.39%	7.61%
5.	EPP_4 (3.125 mg/mL)	92.53%	7.47%
6.	EPP $AgNPs_1$ (25 mg/mL)	86.97%	13.03%
7.	EPP $AgNPs_2$ (12.5 mg/mL)	92.25%	7.75%
8.	EPP $AgNPs_3$ (6.25 mg/mL)	93.32%	6.68%
9.	EPP $AgNPs_4$ (3.125 mg/mL)	94.57%	5.43%

Values are mean percentages of five individual samples from each group (n = 5).

way. Our findings revealed that the ethanolic and methanolic extracts of *P. pavonica* showed a shift in colour from light greenish colour to yellow and translucent, respectively when incubated with silver nitrate and this could reflect the formation of AgNPs [54,55]. We found SPR peaks of AgNPs synthesized from ethanolic and methanolic extracts at 414 nm and 419 nm. Previously, several studies also indicated that the SPR peaks of AgNPs between 380 to 440 nm [17,56,57]. The findings of zeta potential and DLS analysis of ethanolic and methanolic extracts of *P. pavonica* indicated that the synthesized AgNPs showed electrostatic repulsions and uniform size distribution, respectively. The negative zeta potential value of AgNPs might be associated with capping efficacy of bioactive compounds in algal ethanolic and methanolic extracts and which eventually led to stable AgNPs with low agglomeration activity [58,59]. FTIR analysis revealed promising capping agents in algal extracts either alone or in combination with AgNPs. FTIR spectrum of AgNPs fabricated from ethanolic and methanolic algal extracts showed peaks corresponding to phenolic compounds, aromatic compounds, and carbonyl groups. In addition, alkene, aromatic and amide groups were also present in the biogenic AgNPs synthesized from ethanolic and methanolic extracts and suggestive of proteins [55]. The bioactive agents present in the algal based AgNPs could be associated with bio-reduction of silver nitrate and stability of AgNPs [60]. Further, XRD, SEM and EDS analysis revealed the crystalline and spherical shape of AgNPs without impurities accordingly. GC-MS analysis is a powerful technique to characterize bioactive compounds.

Table 6. Molecular docking analysis of 2,4-Di-*tert*-butylphenol and chalcone against selected proteins of bacteria and fungi, respectively.

Protein (Organism, PDB ID, Chain)	Binding affinity (kcal/mol)	Key interacting amino acid residues
Ligand: DTBP *vs*		
Staphylococcus aureus protein (2W9H)	–6.9	Leu5 (H-bond, C–H), Val6 (C–H), Leu28 (alkyl), Val31 (Pi–alkyl), Phe92 (Pi–Pi, Pi–alkyl), Phe98 (Pi–alkyl)
Bacillus subtilis protein (6UF6, A-chain)	–7.7	Gly219 (H-bond), Val69, Val92, Ile71, Ile88, Thr99, Ile257, Gln268, Gln270 (hydrophobic); van der Waals
Pseudomonas aeruginosa protein (6SPC, B-chain)	–5.9	Asp153 (H-bond), Tyr91 (Pi–alkyl), Lys152 (Pi–cation), Ala85, Arg86, Gly88, Met89, Pro90, Gly150 (van der Waals)
S. typhi protein (3FHV, A-chain)	–6.2	Asn180 (H-bond, Pi–sigma), Ile47 (alkyl, Pi–alkyl), Met50, Lys51, Phe110, Asn111, Asn112, Phe114, Gly138, Tyr179
Ligand: Chalcone *vs*		
Candida albicans protein (1NMT, A-chain)	–7.6	Gly413 (H-bond), Tyr225, Phe240 (Pi–Pi), Asp111, Asp112, Phe115, His227, Gly411, Asp412

DTBP and chalcone were selected as ligands based on GC-MS analysis, wherein DTBP was present in both the extracts of *P. pavonica*, while chalcone was alone present in methanolic extracts of *P. pavonica*. DTBP, 2,4-Di-*tert*-butylphenol; GC-MS, gas chromatography-mass spectroscopy.

In the ethanolic and methanolic extracts of *P. pavonica,* we found significant compounds like methyl salicylate, a compound that mediate resistance factor in plants against stress conditions, antimicrobial compounds such as 2,4-di-tert butylphenol, tetradecane, hexadecane and *n*-hexadecanoic acid which can be harmful to the growth of bacteria, and bioactive compounds such as *n*-hexadecanoic acid, ethyl ester and diterpene, Neophytadiene which are possibly associated with antioxidant, anti-inflammatory and anti-microbial activities [61,62] and octadecanoic acid, a bioactive compound with antitumor activity [63].

In the present study, we found antibacterial, antioxidant and antidiabetic properties of AgNPs generated from ethanolic and methanolic extracts of *P. pavonica*. Biofabricated AgNPs prepared from ethanolic and methanolic extracts of *P. pavonica* exhibited antibacterial activity and is in agreement with previous reports [64,65]. The inhibition effect of *P. pavonica* AgNPs prepared from various solvents varied between bacteria to bacteria and could be attributed to the cell membrane of bacteria and depend on the extracted phytochemicals from *P. pavonica* in ethanol and methanol. Though, the exact mechanism of action of antibacterial activity was not determined from this study, the possible mechanism of action of AgNPs could be attributed to (a) disruption of bacterial cell membrane architecture, and enhanced permeability thereby cell death [66,67] and (b) the ability of AgNPs to penetrate the cell wall and target gene expression and proteins which are involved in bacterial metabolism [68]. In view of the development of antimicrobial resistance by bacteria, identification of antibacterial agents with no side effects is of paramount importance. Hence, the present findings might be helpful to develop antibacterial agents.

Antifungal activity of AgNPs generated from methanolic algal extracts was another important finding of this study. Published reports have shown that the AgNPs induced degradation of structural integrity of cell wall might be associated with wrinkling of spores and mycelia, which eventually inactivate the respiratory bound enzymes thereby cell lysis [69,70]. Further, it has been shown that the AgNPs after entering into the fungal environment increase osmotic pressure due to elevated cell membrane permeability resulting in excess water entering the cells [70]. These events might be resulted in exudation of the cellular contents.

In order to get molecular insights to understand the antibacterial and antifungal activities, molecular docking studies were performed. Towards this end, we selected proteins that play essential role in physiological framework of Gram-positive (PDB IDs: 2W9H and 6UF6) and Gram-negative (PDB IDs: 6SPC and 3FHV) bacteria and also yeast, *C. albicans* (PDB ID: 1NMT). *S. aureus* is a

major nosocomial pathogen with rising resistance to diaminopyrimidine inhibitors targeting dihydrofolate reductase (DHFR), a key enzyme in nucleotide biosynthesis. In this study, molecular docking analysis revealed that DTBP from *P. pavonica* binds effectively to the S1 DHFR (PDB ID: 2W9H) of *S. aureus*, suggesting its potential to impair nucleotide synthesis and inhibit bacterial growth. DTBP also exhibited strong interactions with the Longest Common Prefix (LCP) (TagU/TauG family) proteins, which mediate the attachment of teichoic acid polymers to peptidoglycan and are essential for cell wall assembly in Gram-positive bacteria (*B. subtilis* and *S. aureus*) indicating a possible blockade of teichoic acid ligation and disruption of cell wall biosynthesis. In *S. typhi*, DTBP engaged critical residues of the type IVb pilus, a key adhesion factor interacting with Cystic Fibrosis Transmembrane Conductance Regulator (CFTR), implying potential interference with pilus-mediated host cell attachment. Furthermore, DTBP targeted functionally important residues of the ribosomal protein and rRNA binding sites in *P. aeruginosa*, suggesting disruption of ribosome assembly and inhibition of protein synthesis. Collectively, these findings demonstrate that DTBP can modulate multiple essential biochemical pathways across diverse bacterial pathogens, highlighting its promise as a multi-target antimicrobial lead compound. Given the antifungal activity of methanolic extracts of *P. pavonica*, chalcones identified via GC-MS were selected as small-molecule ligands to evaluate their interaction with *Candida albicans* N-myristoyl transferase (PDB ID: 1NMT), an enzyme that catalyzes the transfer of myristate from myristoyl-CoA to the N-terminal glycine of substrate proteins. Molecular docking analysis indicated that chalcone binds to key residues within the active site of 1NMT, suggesting inhibition of its enzymatic activity and potential suppression of yeast vegetative growth.

Finally, to conclude, the rise of antibiotic-resistant pathogens poses a significant threat to modern medicine, highlighting the need for novel agents capable of targeting multiple essential pathways in bacteria and fungi. Molecular docking studies explored their potential antibacterial and antifungal activities wherein the ligand–protein binding patterns observed in this study provide mechanistic insights based on their ability to interact with key proteins and disrupt essential biochemical processes such as nucleotide synthesis, cell wall biosynthesis, host adhesion, and protein translation. Thus, the potential of these compounds as promising candidates for further biological and therapeutic evaluation [71]. Further studies are warranted to validate these compounds and advance their development as therapeutic agents.

Oxidative stress is one of the etiological factors that underlie several pathological conditions and hence, a homeostasis between pro- and antioxidants in cellular systems is of prime concern. Therefore, an imbalance at this level may cause oxidative stress induced damage to cells/tissues. It is well accepted that the plants including macro algae are rich sources of bioactive compounds with antioxidant properties and thus, probing and identification of compounds that are safe and sustain the cellular antioxidant system is a part of biomedical research [72]. In this study, we evaluated the antioxidant efficacy of AgNPs produced from ethanolic and methanolic extracts of *P. pavonica* through *in vitro* experiments. Bio-fabricated AgNPs showed DPPH scavenging activity suggesting that the NPs can able to quench the free radicals directly and indicate antioxidant property. This could be ascribed to the ability of plant-based AgNPs to donate hydrogen atoms. Further, we found a significant reduction in the superoxide ions was observed in the presence of bio-fabricated AgNPs suggesting scavenging activity against lipid peroxidation induced free radicals and this activity may be helpful to protect cells/tissues against oxidative damage [73]. Significant elevation in TAC activities of AgNPs synthesized from ethanolic and methanolic extracts of *P. pavonica* could be due to the occurrence of phenolic and flavonoids. Further, the TAC activity was greater as compared to their respective controls i.e., ethanolic and methanolic extracts alone and could be ascribed to the distribution of bioactive compounds at the nano-level by AgNPs synthesized from ethanolic and methanolic extracts of *P. pavonica*. The results are in agreement with previous studies [17,64,65]. Recent studies of Bharath et al. [74] suggested that the lipophilic compounds like *n*-hexadecanoic acid from brown algae *Turbinaria ornate* showed antioxidant as indicated by DPPH radical scavenging activity and also exhibited anticancer properties.

Development of therapeutic strategies to overcome non-insulin mediated diabetes is one of the emerging areas of biomedicine [72]. Studies have shown that the α-glucosidase or brush border enzyme plays an essential enzyme in mediating the conversion of starch and disaccharides into glucose which in turn absorbed by the enterocytes of small intestine [75,76]. Thus, inhibition of α-glucosidase activity can be associated with delay in digestion of carbohydrates and lower glucose levels in blood [77,78] and could be used as a therapeutic strategy to overcome non-insulin mediated diabetes. In the current study, AgNPs bio-fabricated with ethanolic and methanolic extracts of *P. pavonica* showed inhibitory effects against α-glucosidase enzyme and might be ascribed to their bioactive compounds in *P. pavonica* [79,80,81]. TM3 cell lines were selected in this study because they reflect mice Leydig cells. Since, *P. pavonica* exhibit reproductive efficacy, we investigated its biocompatibility and cytotoxic effects on TM3 cell lines. Interestingly, the MTT assay results suggested that lower concentrations of the crude extract were biocompatible and minimally cytotoxic. This aligns with literature on green-synthesized nanoparticles, which often show improved biocompatibility, enhanced stability, and reduced sedimentation [82].

Limitations

However, further *in vivo* validation and mechanistic studies to facilitate translational and clinical applications are warranted. Despite of this limitation, these findings establish *P. pavonica* as a robust and versatile biological platform for the green synthesis of multifunctional AgNPs.

5. Conclusion

In the present investigation, a sustainable and environmentally benign green synthesis strategy was established for the fabrication of AgNPs using ethanolic and methanolic extracts of the marine brown alga *Padina pavonica*. Particle selection based on DLS and zeta potential analyses confirmed the formation of highly stable AgNPs with favourable nanoscale dimensions and electrostatic repulsion. FTIR spectroscopy identified the phytochemical functional groups which could be linked to the bio-reduction of silver ions suggesting capping efficacy of biogenic nanoparticles. Comprehensive physicochemical characterization using SEM, EDS, and XRD further validated the crystalline nature, elemental composition, and predominantly spherical morphology of the phyto-fabricated AgNPs.

Functionally, AgNPs synthesized from both the extracts of ethanol and methanol exhibited multifaceted biological (antioxidant, antibacterial and antidiabetic) activities, highlighting their broad-spectrum therapeutic potential. Notably, antifungal activity was exclusively observed in methanolic extract–mediated AgNPs, suggesting solvent-dependent phytochemical incorporation and differential biofunctionalization of the nanoparticle surface. This selective antifungal efficacy may be correlated to the enhanced presence or availability of antifungal secondary metabolites in the methanolic extract, underscoring the critical role of extraction chemistry in modulating nanoparticle bioactivity.

It is noteworthy that *in vitro* cell viability and cytotoxicity assessments demonstrated high biocompatibility of the synthesized AgNPs, particularly at lower concentrations, reinforcing their suitability for biomedical applications. The demonstrated antimicrobial, antioxidant and antidiabetic properties, coupled with favourable biocompatibility, position these bio-synthesized AgNPs as promising candidates for advanced nanotherapeutic development.

Availability of Data and Materials

All data generated or analysed during this study are included in this published article and its supplementary information files.

Author Contributions

NVM and KVN: Writing - original draft, Validation, Software, Methodology, Investigation, Formal analysis, Data curation. PN: conducted the in-silico analysis. RU: Supervision, Investigation, Formal analysis, Conceptualization. SBS: Writing – review & editing, Writing – original draft, Supervision, Investigation, Formal analysis, Conceptualization. BK: Writing – review & editing, Validation, Supervision, Project administration, Formal analysis, Conceptualization. All authors contributed to editorial changes in the manuscript. All authors read and approved the final manuscript. All authors have participated sufficiently in the work and agreed to be accountable for all aspects of the work.

Ethics Approval and Consent to Participate

Not applicable.

Acknowledgment

The authors are thankful to the Head, Department of Biotechnology, Sri Padmavati Mahila Visvavidyalayam, Tirupati for providing the laboratory facilities. Authors also thankful to DST-CURIE Central instrumentation facility, Sri Padmavati Mahila Visvavidyalayam, Tirupati. Authors also thank the Head, Dept. of Food Technology, VS University for providing laboratory facilities.

Funding

The authors are thankful for the financial support received under PM-USHA-MERU granted to Sri Padmavati Mahila Visvavidyalayam, Tirupati, A.P. Research project sanctioned to Dr. Battini Kishori, (Professor, Department of Biotechnology), R.O.C.No.SPMVV/UGC/F1/PM-USHA/2024, Dated: 31-12-2024.

Conflicts of Interest

The authors declare no conflicts of interest.

Supplementary Material

Supplementary material associated with this article can be found, in the online version, at https://doi.org/10.31083/DJNB51994.

References

[1] Laxmi V, Singhvi N, Ahmad N, Sinha S, Negi T, Gupta V, et al. Emerging Field of Nanotechnology in Environment. Indian Journal of Microbiology. 2023; 63: 244–252. https://doi.org/10.1007/s12088-023-01092-7

[2] Xu L, Wang YY, Huang J, Chen CY, Wang ZX, Xie H. Silver nanoparticles: Synthesis, medical applications and biosafety. Theranostics. 2020; 10: 8996–9031. https://doi.org/10.7150/thno.45413

[3] Wu J, Yue X, Wang T, Zhang Y, Jin Y, Li G. A cost-effective and sensitive voltammetric sensor for determination of baicalein in herbal medicine based on shuttle-shape α-Fe2O3 nanoparticle decorated multi-walled carbon nanotubes. Colloids and Surfaces A: Physicochemical and Engineering Aspects. 2025; 717: 136850. https://doi.org/10.1016/j.colsurfa.2025.136850

[4] Kanwar S, Vijayavenkataraman S. 3D-printed polycaprolactone-magnetic nanoparticles composite multifunctional scaffolds for bone tissue regeneration and

hyperthermia treatment. International Journal of Bioprinting. 2024; 10: 4538. https://doi.org/10.36922/ijb.4538

[5] Guo X, Zheng Q, Gao W, Xiao Y, Shi L, Lin F, et al. Synergistic microglial modulation by laminarin-based platinum nanozymes for potential intracerebral hemorrhage therapy. Biomaterials. 2025; 319: 123212. https://doi.org/10.1016/j.biomaterials.2025.123212

[6] Wang X, Sun K, Dong J, Ge Y, Liu H, Jin X, et al. Carrier-free nanoparticles based on natural products trigger dual "synergy and attenuation" for enhanced phototherapy of liver cancer. Materials Today. Bio. 2025; 35: 102278. https://doi.org/10.1016/j.mtbio.2025.102278

[7] Lu JY, Bu ZQ, Lei YQ, Wang D, He B, Wang J, et al. Facile microwave-assisted synthesis of Sb2O3-CuO nanocomposites for catalytic degradation of p-nitrophenol. Journal of Molecular Liquids. 2024; 409: 125503. https://doi.org/10.1016/j.molliq.2024.125503

[8] Nasrollahzadeh M, Sajadi SM, Sajjadi M, Issaabadi Z. An introduction to nanotechnology. Interface Science and Technology (pp. 1–27). Elsevier: Amsterdam, Netherlands. 2019. https://doi.org/10.1016/B978-0-12-813586-0.00001-8

[9] Alharbi NS, Alsubhi NS, Felimban AI. Green synthesis of silver nanoparticles using medicinal plants: Characterization and application. Journal of Radiation Research and Applied Sciences. 2022; 15: 109–124. https://doi.org/10.1016/j.jrras.2022.06.012

[10] Karunakaran G, Sudha KG, Ali S, Cho EB. Biosynthesis of Nanoparticles from Various Biological Sources and Its Biomedical Applications. Molecules (Basel, Switzerland). 2023; 28: 4527. https://doi.org/10.3390/molecules28114527

[11] Hou J, Gong H, Gong Z, Tan X, Qin X, Nie J, et al. Structural characterization and anti-inflammatory activities of a purified polysaccharide from fruits remnants of Alpinia zerumbet (Pers.) Burtt. et Smith. International Journal of Biological Macromolecules. 2024; 267: 131534. https://doi.org/10.1016/j.ijbiomac.2024.131534

[12] Gong H, Tan X, Hou J, Gong Z, Qin X, Nie J, et al. Separation, purification, structure characterization, and immune activity of a polysaccharide from Alocasia cucullata obtained by freeze-thaw treatment. International Journal of Biological Macromolecules. 2024; 282: 137232. https://doi.org/10.1016/j.ijbiomac.2024.137232

[13] Chang M, Liu K, Zhu G, Gul P, Khan J. Structural characterization and hypoglycaemic effects on type 2 diabetic mice of Spirulina platensis polysaccharides and Se-modified polysaccharides. Food Bioscience. 2025; 64: 105826. https://doi.org/10.1016/j.fbio.2025.105826

[14] Zu-Man D, Yu-Long Z, Chun-Yang T, Chuang L, Jia-Qin F, Qiang H, et al. Construction of blackberry polysaccharide nanoselenium particles: Structure features and regulation effects of glucose/lipid metabolism in HepG2 cells. Food Research International (Ottawa, Ont.). 2024; 187: 114428. https://doi.org/10.1016/j.foodres.2024.114428

[15] Hosny S, Gaber GA, Ragab MS, Ragheb MA, Anter M, Mohamed LZ. A Comprehensive Review of Silver Nanoparticles (AgNPs): Synthesis Strategies, Toxicity Concerns, Biomedical Applications, AI-Driven Advancements, Challenges, and Future Perspectives. Arabian Journal for Science and Engineering. 2025; 51: 13667–13714. https://doi.org/10.1007/s13369-025-10612-0

[16] Junaid M, Soomro HA, Ahmad AQ, Faiz S, Shahid NA, Al-Rawi MB, et al. A Green Approach to Silver Nanoparticle Synthesis Using Glycyrrhiza glabra to Investigations Antimicrobial Applications. International Journal of Chemical Kinetics. 2025; 57: 426–433 https://doi.org/10.1002/kin.21787

[17] Mrunalini NV, Deepthi PN, Kishori B, Sainath SB. Biogenic synthesis of silver nanoparticles using methanolic extracts of Ulva lactuca: GC/MS analysis, antibacterial, antioxidant, and antidiabetic activity. Next Materials. 2025; 9: 100923. https://doi.org/10.1016/j.nxmate.2025.100923

[18] Wang Q, Feng S, Zhong L, Zhou Y, Liu J, Liu H, et al. Polydopamine-functionalized cellulose nanofibrils with Ag deposition for robust poly(vinyl alcohol) hydrogel strain sensor. International Journal of Biological Macromolecules. 2026; 347: 150776. https://doi.org/10.1016/j.ijbiomac.2026.150776

[19] Benita M, Dubinsky Z, Iluz D. Padina pavonica: Morphology and calcification functions and mechanism. American Journal of Plant Sciences. 2018; 9: 1156–1168. https://doi.org/10.4236/ajps.2018.96087

[20] Orlando-Bonaca M, Pitacco V, Bajt O, Falnoga I, Hudobivnik MJ, Mazej D, et al. Spatial and temporal distribution of trace elements in Padina pavonica from the northern Adriatic Sea. Marine Pollution Bulletin. 2021; 172: 112874. https://doi.org/10.1016/j.marpolbul.2021.112874

[21] Ansari AA, Ghanem SM, Naeem M. Brown alga Padina: a review. International Journal of Botany Studies. 2019; 4: 01–03.

[22] Hlila MB, Hichri AO, Mahjoub MA, Mighri Z, Mastouri M. Antioxidant and Antimicrobial Activities of Padina Pavonica and Enteromorpha Sp. from the Tunisian Mediterranean Coast. Journal of Coastal Life Medicine. 2017; 5: 336–342. https://doi.org/10.12980/jclm.5.2017J7-107

[23] Bernardini G, Minetti M, Polizzotto G, Biazzo M, Santucci A. Pro-Apoptotic Activity of French Polynesian *Padina pavonica* Extract on Human Osteosarcoma Cells. Marine Drugs. 2018; 16: 504. https://doi.org/10.3390/md16120504

[24] Al-Enazi NM, Awaad AS, Zain ME, Alqasoumi SI. Antimicrobial, antioxidant and anticancer activities of *Laurencia catarinensis*, *Laurencia majuscula* and *Padina pavonica* extracts. Saudi Pharmaceutical Journal: SPJ: the Official Publication of the Saudi Pharmaceutical Society. 2018; 26: 44–52. https://doi.org/10.1016/j.jsps.2017.11.001

[25] Hidayati JR, Bahry MS, Karlina I, Yudiati E. Antioxidant activity and bioactive compounds of tropical brown algae Padina sp. from Bintan Island, Indonesia. Jurnal Kelautan Tropis. 2022; 25: 309–319. https://doi.org/10.14710/jkt.v25i3.15562

[26] Čagalj M, Skroza D, Tabanelli G, Özogul F, Šimat V. Maximizing the Antioxidant Capacity of Padina pavonica by Choosing the Right Drying and Extraction Methods. Processes. 2021; 9: 587. https://doi.org/10.3390/pr9040587

[27] Mesripour A, Asgari N, Yegdaneh A. The brown alga *Padina pavonica* methanol and hexane partitions prevented depressive behavior induced by dexamethasone in mice. Research in Pharmaceutical Sciences. 2025; 20: 241–249. https://doi.org/10.4103/RPS.RPS_3_24

[28] Cikoš AM, Jokić S, Šubarić D, Jerković I. Overview on the Application of Modern Methods for the Extraction of Bioactive Compounds from Marine Macroalgae. Marine Drugs. 2018; 16: 348. https://doi.org/10.3390/md16100348

[29] Sudha G, Balasundaram A. Determination of Bioactive Components in the Methanolic Extract of Padina pavonica Using GC-MS. World Journal of Pharmaceutical Research. 2018; 7: 991–997. https://doi.org/10.20959/wjpr201812-12725

[30] Amin HH, El-Sayed AB, Ramadan KM, Moussa ZA, Moawad FG. Evaluation of biological activity of extracts from different species of algae. Journal of Biological Chemistry and Environmental Sciences. 2015; 10: 281–297. https://doi.org/10.21608/bces.2015.473993

[31] Aziz N, Fatma T, Varma A, Prasad R. Biogenic synthesis of silver nanoparticles using Scenedesmus abundans and evaluation of their antibacterial activity. Journal of Nanoparticles. 2014; 2014: 689419. https://doi.org/10.1155/2014/689419

[32] Wang L, Hu C, Shao L. The antimicrobial activity of nanoparticles: present situation and prospects for the future. Interna-

tional Journal of Nanomedicine. 2017; 12: 1227–1249. https://doi.org/10.2147/IJN.S121956
[33] Mallmann EJJ, Cunha FA, Castro BNMF, Maciel AM, Menezes EA, Fechine PBA. Antifungal activity of silver nanoparticles obtained by green synthesis. Revista do Instituto De Medicina Tropical De Sao Paulo. 2015; 57: 165–167. https://doi.org/10.1590/S0036-46652015000200011
[34] Hashem AH, Saied E, Amin BH, Alotibi FO, Al-Askar AA, Arishi AA, et al. Antifungal Activity of Biosynthesized Silver Nanoparticles (AgNPs) against *Aspergilli* Causing Aspergillosis: Ultrastructure Study. Journal of Functional Biomaterials. 2022; 13: 242. https://doi.org/10.3390/jfb13040242
[35] Yamaguchi T, Takamura H, Matoba T, Terao J. HPLC method for evaluation of the free radical-scavenging activity of foods by using 1,1-diphenyl-2-picrylhydrazyl. Bioscience, Biotechnology, and Biochemistry. 1998; 62: 1201–1204. https://doi.org/10.1271/bbb.62.1201
[36] Prior RL, Wu X, Schaich K. Standardized methods for the determination of antioxidant capacity and phenolics in foods and dietary supplements. Journal of Agricultural and Food Chemistry. 2005; 53: 4290–4302. https://doi.org/10.1021/jf0502698
[37] Nishikimi M, Appaji N, Yagi K. The occurrence of superoxide anion in the reaction of reduced phenazine methosulfate and molecular oxygen. Biochemical and Biophysical Research Communications. 1972; 46: 849–854. https://doi.org/10.1016/s0006-291x(72)80218-3
[38] Ahmed D, Baig H, Zara S. Seasonal variation of phenolics, flavonoids, antioxidant and lipid peroxidation inhibitory activity of methanolic extract of Melilotus indicus and its sub-fractions in different solvents. International Journal of Phytomedicine. 2012; 4: 326–332.
[39] Dewi RT, Iskandar YM, Hanafi M, Kardono LBS, Angelina M, Dewijanti ID, et al. Inhibitory effect of koji Aspergillus terreus on alpha-glucosidase activity and postprandial hyperglycemia. Pakistan Journal of Biological Sciences: PJBS. 2007; 10: 3131–3135. https://doi.org/10.3923/pjbs.2007.3131.3135
[40] Wypij M, Jędrzejewski T, Trzcińska-Wencel J, Ostrowski M, Rai M, Golińska P. Green Synthesized Silver Nanoparticles: Antibacterial and Anticancer Activities, Biocompatibility, and Analyses of Surface-Attached Proteins. Frontiers in Microbiology. 2021; 12: 632505. https://doi.org/10.3389/fmicb.2021.632505
[41] Al-Khedhairy AA, Wahab R. Silver nanoparticles: An instantaneous solution for anticancer activity against human liver (HepG2) and breast (MCF-7) cancer cells. Metals. 2022; 12: 148. https://doi.org/10.3390/met12010148
[42] Abbasi S, İlhan A, Jabbari H, Javidzade P, Safari M, Abolhasani Zadeh F. Cytotoxicity evaluation of synthesized silver nanoparticles by a Green method against ovarian cancer cell lines. Nanomedicine Research Journal. 2022; 7: 156–164. https://doi.org/10.22034/nmrj.2022.02.005
[43] Zhao F, Wang P, Lucardi RD, Su Z, Li S. Natural Sources and Bioactivities of 2,4-Di-Tert-Butylphenol and Its Analogs. Toxins. 2020; 12: 35. https://doi.org/10.3390/toxins12010035
[44] Yeye EO, AkintundeAdeniyi-Akee M, Ahmed SA, Aboaba SA. In silico studies and antimicrobial investigation of synthesised novel N-acylhydrazone derivatives of indole. Scientific African. 2023; 19: e01463. https://doi.org/10.1016/j.sciaf.2022.e01463
[45] Hastuti LP, Hermawan F, Prastya ME, Ernawati T, Putra NR, Jumina J, et al. In-silico and in-vitro study of hydroxythioxanthone derivatives as a potential candidate for antibacterial agents. Results in Chemistry. 2025; 17; 102525. https://doi.org/10.1016/j.rechem.2025.102525
[46] Gupta D, Jain DK. Chalcone derivatives as potential antifungal agents: Synthesis, and antifungal activity. Journal of Advanced Pharmaceutical Technology & Research. 2015; 6: 114–117. https://doi.org/10.4103/2231-4040.161507
[47] Meenambiga SS, Rajagopal K. Antibiofilm activity and molecular docking studies of bioactive secondary metabolites from endophytic fungus Aspergillus nidulans on oral Candida albicans. Journal of Applied Pharmaceutical Science. 2018; 8: 037–045. https://dx.doi.org/10.7324/JAPS.2018.8306
[48] Harborne JB. Phytochemical Methods: A Guide to Modern Techniques of Plant Analysis. Chapman and Hall: London. 1973.
[49] Markham KR. Techniques of Flavonoid Identification. Academic Press: London. 1982.
[50] Sofowora A. Medicinal Plants and Traditional Medicine in Africa. Spectrum Books Ltd.: Ibadan, Nigeria. 1993.
[51] Trease GE, Evans WC. Pharmacognosy. 15th edn. Saunders Publishers: London. 2002.
[52] Benedict SR. A reagent for the detection of reducing sugars. Journal of Biological Chemistry. 1909; 5: 485–487. https://doi.org/10.1016/S0021-9258(18)91645-5
[53] Gornall AG, Bardawill CJ, David MM. Determination of serum proteins by means of the biuret reaction. The Journal of Biological Chemistry. 1949; 177: 751–766. https://doi.org/10.1016/S0021-9258(18)57021-6
[54] Dixit D, Gangadharan D, Popat KM, Reddy CRK, Trivedi M, Gadhavi DK. Synthesis, characterization and application of green seaweed mediated silver nanoparticles (AgNPs) as antibacterial agents for water disinfection. Water Science and Technology: a Journal of the International Association on Water Pollution Research. 2018; 78: 235–246. https://doi.org/10.2166/wst.2018.292
[55] Rajivgandhi GN, Ramachandran G, Maruthupandy M, Manoharan N, Alharbi NS, Kadaikunnan S, et al. Anti-oxidant, antibacterial and anti-biofilm activity of biosynthesized silver nanoparticles using Gracilaria corticata against biofilm producing K. pneumoniae. Colloids and Surfaces A: Physicochemical and Engineering Aspects. 2020; 600: 124830. https://doi.org/10.1016/j.colsurfa.2020.124830
[56] Edison TJ, Sethuraman MG. Instant green synthesis of silver nanoparticles using Terminalia chebula fruit extract and evaluation of their catalytic activity on reduction of methylene blue. Process Biochemistry. 2012; 47: 1351–1357. http://dx.doi.org/10.1016/j.procbio.2012.04.025
[57] Sivaraman D, Panneerselvam P, Muralidharan P, Prabhu TP, Kumar RV. Green synthesis, characterization and anti-microbial activity of silver nanoparticles produced using Ipomoea aquatica forsk leaf extract. International Journal of Pharmaceutical Sciences and Research. 2013; 4: 2280. http://dx.doi.org/10.13040/IJPSR.0975-8232.4(6).2280-85
[58] Niraimathi KL, Sudha V, Lavanya R, Brindha P. Biosynthesis of silver nanoparticles using Alternanthera sessilis (Linn.) extract and their antimicrobial, antioxidant activities. Colloids and Surfaces. B, Biointerfaces. 2013; 102: 288–291. https://doi.org/10.1016/j.colsurfb.2012.08.041
[59] Chugh D, Viswamalya VS, Das B. Green synthesis of silver nanoparticles with algae and the importance of capping agents in the process. Journal, Genetic Engineering & Biotechnology. 2021; 19: 126. https://doi.org/10.1186/s43141-021-00228-w
[60] Asif M, Yasmin R, Asif R, Ambreen A, Mustafa M, Umbreen S. Green Synthesis of Silver Nanoparticles (AgNPs), Structural Characterization, and their Antibacterial Potential. Dose-response: a Publication of International Hormesis Society. 2022; 20: 15593258221088709. https://doi.org/10.1177/15593258221088709
[61] Liaqat N, Jahan N, Anwar T, Qureshi H. Green synthesized silver nanoparticles: Optimization, characterization, antimicrobial activity, and cytotoxicity study by hemolysis assay. Frontiers in Chemistry. 2022; 10: 952006. https://doi.org/10.3389/fchem.

2022.952006
[62] Nisa S, Bibi Y, Masood S, Ali A, Alam S, Sabir M, et al. Isolation, Characterization and Anticancer Activity of Two Bioactive Compounds from *Arisaema flavum* (Forssk.) Schott. Molecules (Basel, Switzerland). 2022; 27: 7932. https://doi.org/10.3390/molecules27227932
[63] Sudharsan S, Saravanan R, Shanmugam A, Vairamani S, Kumar RM, Menaga S, Ramesh N. Isolation and Characterization of Octadecanoic Acid from The Ethyl Acetate Root Extract of Trigonella foneum graecum L. by Using Hydroponics Method. Bioterrorism & Biodefense. 2011; 2: 105. http://dx.doi.org/10.4172/2157-2526.1000105
[64] Khodeer DM, Nasr AM, Swidan SA, Shabayek S, Khinkar RM, Aldurdunji MM, et al. Characterization, antibacterial, antioxidant, antidiabetic, and anti-inflammatory activities of green synthesized silver nanoparticles using *Phragmanthera austroarabica* A. G. Mill and J. A. Nyberg extract. Frontiers in Microbiology. 2023; 13: 1078061. https://doi.org/10.3389/fmicb.2022.1078061
[65] Choudhary S, Sangela V, Saxena P, Saharan V, Pugazhendhi A, Harish. Recent progress in algae-mediated silver nanoparticle synthesis. International Nano Letters. 2023; 13: 193–207. https://doi.org/10.1007/s40089-022-00390-0
[66] More PR, Pandit S, Filippis AD, Franci G, Mijakovic I, Galdiero M. Silver Nanoparticles: Bactericidal and Mechanistic Approach against Drug Resistant Pathogens. Microorganisms. 2023; 11: 369. https://doi.org/10.3390/microorganisms11020369
[67] Bhuyar P, Rahim MH, Sundararaju S, Ramaraj R, Maniam GP, Govindan N. Synthesis of silver nanoparticles using marine macroalgae Padina sp. and its antibacterial activity towards pathogenic bacteria. Beni-Suef University Journal of Basic and Applied Sciences. 2020; 9: 1–15. https://doi.org/10.1186/s43088-019-0031-y
[68] Mikhailova EO. Silver Nanoparticles: Mechanism of Action and Probable Bio-Application. Journal of Functional Biomaterials. 2020; 11: 84. https://doi.org/10.3390/jfb11040084
[69] Xia ZK, Ma QH, Li SY, Zhang DQ, Cong L, Tian YL, et al. The antifungal effect of silver nanoparticles on Trichosporon asahii. Journal of Microbiology, Immunology, and Infection = Wei Mian Yu Gan Ran Za Zhi. 2016; 49: 182–188. https://doi.org/10.1016/j.jmii.2014.04.013
[70] Gordienko MG, Palchikova VV, Kalenov SV, Belov AA, Lyasnikova VN, Poberezhniy DY, et al. Antimicrobial activity of silver salt and silver nanoparticles in different forms against microorganisms of different taxonomic groups. Journal of Hazardous Materials. 2019; 378: 120754. https://doi.org/10.1016/j.jhazmat.2019.120754
[71] Rouvier F, Abou L, Wafo E, Andre P, Cheyrol J, Khacef MM, et al. Identification of 2,4-di-tert-butylphenol as an antimicrobial agent against Cutibacterium acnes bacteria from Rwandan propolis. Antibiotics. 2024; 13: 1080. https://doi.org/10.3390/antibiotics13111080
[72] Monroy-García IN, Torres-Romero S, Castro-Ochoa LD, Mendoza-Acosta A, Viveros-Valdez E, Ayala-Zavala F. Bioactive compounds from marine macroalgae: A natural defense against oxidative stress-related diseases. Stresses. 2025; 5: 22. https://doi.org/10.3390/stresses5010022
[73] Matin M, Koszarska M, Atanasov AG, Król-Szmajda K, Jóźwik A, Stelmasiak A, et al. Bioactive Potential of Algae and Algae-Derived Compounds: Focus on Anti-Inflammatory, Antimicrobial, and Antioxidant Effects. Molecules (Basel, Switzerland). 2024; 29: 4695. https://doi.org/10.3390/molecules29194695
[74] Bharath B, Perinbam K, Devanesan S, AlSalhi MS, Saravanan M. Evaluation of the anticancer potential of Hexadecenoic acid from brown algae Turbinaria ornata on HT–29 colon cancer cells. Journal of Molecular Structure. 2021; 1235: 130229. https://doi.org/10.1016/j.molstruc.2021.130229
[75] Elferink H, Bruekers JPJ, Veeneman GH, Boltje TJ. A comprehensive overview of substrate specificity of glycoside hydrolases and transporters in the small intestine: "A gut feeling". Cell Mol Life Sci. 2020; 77: 4799–4826. https://doi.org/10.1007/s00018-020-03564-1
[76] Kashtoh H, Baek KH. Recent updates on phytoconstituent alpha-glucosidase inhibitors: An approach towards the treatment of type two diabetes. Plants (Basel). 2022; 11: 2722. https://doi.org/10.3390/plants11202722
[77] Andreadi A, Lodeserto P, Todaro F, Meloni M, Romano M, Minasi A, et al. Nanomedicine in the Treatment of Diabetes. International Journal of Molecular Sciences. 2024; 25: 7028. https://doi.org/10.3390/ijms25137028
[78] AG HBB. Pharmacology of alpha-glucosidase inhibition. European Journal of Clinical Investigation. 1994; 24: 3–10. https://doi.org/10.1111/j.1365-2362.1994.tb02249.x
[79] Pistia-Brueggeman G, Hollingsworth RI. A preparation and screening strategy for glycosidase inhibitors. Tetrahedron. 2001; 57: 8773–8778. https://doi.org/10.1016/S0040-4020(01)00877-8
[80] Abideen S, Sankar M. In-vitro screening of antidiabetic and antimicrobial activity against green synthesized AgNO3 using seaweeds. Nanomedicine & Nanotechnology. 2015; 10: 2157–7439. http://dx.doi.org/10.4172/2157-7439.S6-001
[81] Gunathilaka TL, Samarakoon K, Ranasinghe P, Peiris LDC. Antidiabetic Potential of Marine Brown Algae-a Mini Review. Journal of Diabetes Research. 2020; 2020: 1230218. https://doi.org/10.1155/2020/1230218
[82] Zabihi MM, Eghbaliferiz S, Khorashadizadeh M, Mortazavi-Derazkola S, Yousefi M. Green synthesis of non-toxic silver nanoparticles using Salvia tebesana Bunge extract: Optimization, cytotoxicity, and antibacterial activities. Results in Chemistry. 2024; 7: 101510. https://doi.org/10.1016/j.rechem.2024.101510